Case study

Evaluation of the bond-dependent factors for CFRP bars used as structural reinforcement: A critical review

Mohd Basri Che Bakar [a,b,*], Raizal Saifulnaz Muhammad Rashid [a,**], Mugahed Amran [c,d], Mohd Saleh Jaafar [a]

[a] Department of Civil Engineering, Universiti Putra Malaysia, 43400 Serdang, Selangor, Malaysia
[b] Public Works Department Malaysia, 50582 Kuala Lumpur, Malaysia
[c] Department of Civil Eng., College of Eng., Prince Sattam Bin Abdulaziz University, 11942 Alkharj, Saudi Arabia
[d] Department of Civil Engineering, Faculty of Engineering and IT, Amran University, 9677 Amran, Yemen

ABSTRACT

This study analyzes the precious data from the literature on bond strength between concrete and CFRP bars associated with the pullout test. In this regard, an overview of the pullout test and bond stress-slip model, along with a systematic analysis of characteristic bond strength behavior, were reviewed extensively. Over 273 specimens of CFRP bar involved in pullout tests were mined from the experimental works reported by preceding researchers worldwide. Significant findings revealed that the pullout test is a widely used method for determining the bond strength of embedded CFRP bars in concrete. The concrete compressive strength, bar diameter, modulus of elasticity, embedment length and surface treatment all have a major impact on bond performance. Moreover, the development of an analytical model for bond stress-slip is paramount to present the interaction behavior as well as to perform numerical analysis. In addition, bond strength predictions by international guidelines are conservative. However, the bond strength calculated by ACI 440.1R-15 has proven to be more practical across all the statistical measures. In line with this review, recommended research areas are also successfully discussed and proposed for further investigation.

1. Introduction

The corrosion of steel bars is indeed a main cause of deterioration in reinforced concrete (RC) structures. This issue has been frequently recorded for those structures located in the coastal area [1,2]. During the corrosion stage, the reaction between iron (Fe) and its surrounding environment produces corrosion products consisting of various oxides [3–6]. These processes subsequently damage the interface and degrade the bond strength between concrete and steel bars. The preceding reports had stated that bond strength may degrade more than 50% of its original strength when the corrosion level reaches about 6% [7,8]. Consequently, this could cause cracks, delamination and finally spalling of the concrete slab as depicted in Fig. 1 [8]. This corroded reinforcement ultimately affects structural integrity and hence, shorten the lifespan of RC structures [4,9–11]. However, the employment of fiber-reinforced polymer (FRP) in RC structures has become highly imperative [12–21]. For instance, carbon fiber reinforced polymer (CFRP) is a composite material that

includes carbon fibers enmeshed in a resin matrix to dynamically increase a polymer model's stiffness and strength [22]. Specifically, CFRP bars are up to 8 times more resistant than traditional steel reinforcement bar when used to reinforce the RC structures [12]. Henceforward, the utilization of CFRP bars, "as a type of FRP materials" as structural reinforcement has attracted great interest in developing such smart and sustainable RC structures for the past two decades [23–25].

It has been proven that CFRP bars have superior material characteristics for both physical and mechanical properties. CFRP bars relatively have a small diameter (e.g.: in the range of 8–14 mm), exceptional tensile strength (e.g.: up to maximum strength of 3690 MPa), lower elastic modulus than steel bars (e.g.: in the range of 100–180 GPa), noncorrosive and nonmagnetic materials [12,23, 26–30]. In addition, CFRP bars have superior resistance against chemical solutions including saline, acid and alkaline as compared to the other types of fiber [15,31–36]. Moreover, in contrast to steel, CFRP bars behave as anisotropic composite materials, non-homogeneous and linear elastic properties [17,23]. These inherent properties of CFRP bars would significantly affect the bond performances with concrete.

Until now, reliable bond strength test data have been required for the characterization of the wide range of CFRP bars offered by the global industries. Significant variance in material properties of CFRP bar may also contribute to the knowledge gaps. Recent research has indicated that the pullout test has been widely adapted method for determining the bond strength of embedded CFRP bars in concrete [37–40]. Thus, an overview of the pullout test including specimen preparations and experimental procedures, should deliver a better understanding and clearer pictures to the structural engineers on how this test had been conducted.

In relation to that, the bond stress-slip curve was developed from pullout test. The said curve is paramount to present the interaction behavior between CFRP bar and concrete. It is noteworthy that current bond stress-slip models were derived and developed under certain assumptions and considerations. The revolution in the bond stress-slip models have revealed such an improvement in performing numerical analysis and predicting maximum bond strength [41]. A comprehensive review on the available bond stress-slip models are studied and evaluated, exhibit their potential application in the real practice [42,43].

Furthermore, an overview on the current design codes have found that some predictions on bond strength are calculated without considering the factors like embedment length, bar surface treatment, fiber type and transverse reinforcement. For instance, bond strength equations proposed by ACI 440.1R-15 [23] and CSA S806–12 [44] predict the bond strength with the absentee factor of transverse reinforcement. Thus, it is indeed necessary to evaluate the bond strength prediction for embedded CFRP bars in concrete.

In RC structures, bond characteristics for embedded CFRP bars in concrete are fundamental aspect of composite action [45,46]. Narrowing down to the beam applications, the bond between CFRP bars and concrete is vital in transmitting stresses [27,39,45,47,48]. Also, adequate bond strength may increase the beam stiffness prior to achieve its ultimate moment capacity and subsequently reduce the cracks width and deflections [17,32,49,50]. Having these significant effects, identifying the factors affecting the bond strength of embedded CFRP bars in concrete is paramount [17]. Numerous researchers had concluded that the major factors affecting the bond strength between concrete and CFRP bars can be summarized into three headings [48,51–55]. There are: (i) properties of CFRP bars; (ii) arrangement and configuration of CFRP bars; and, (iii) properties of concrete [26,27,29,32,36,56,57]. The specific factors under these three headings are summarized in Fig. 2. For the sake of clarity, parametric studies on bond characteristics are then conducted throughout this review to investigate the relationships between all those factors.

With the persistence of analyzing the most precious data from the literatures, this paper aims to deliver a comprehensive review on the important aspects of bond dependent-factors for embedded CFRP bars in concrete. In accordance with the study's aim, this paper also discusses about the related issues regarding the experimental works and bond strength prediction. Hence, the structure of this paper is as follows. A brief summary on the pullout test in terms of specimen preparations and experimental procedures are presented in Section 2. Section 3 discusses on the existing of four bond stress-slip models for embedded concrete with CFRP bars. Both of their merits and drawbacks in predicting bond behavior are effectively compared. Furthermore, Section 4 revises on the bond strength predictions by international design provisions. Also, comparisons between the predicted and experimental bond strength are covered and well discussed in this section. Parametric investigation is covered in Section 5 on the key factors affecting the characteristic bond behavior between CFRP bar and concrete. Failure mode, bond strength and corresponding slip are analysed throughout the statistical analysis based on the experimental database. Towards the end of this paper, Section 6 discusses about the recommended research areas that can be considered for future studies. Conclusion are finally drawn in Section 7.
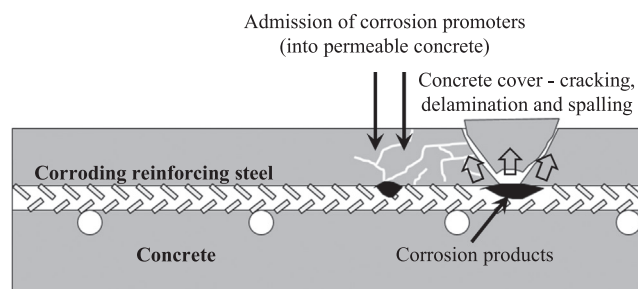

Fig. 1. Corrosion of steel reinforcement at soffit slab causing concrete deterioration (modified from [8]).
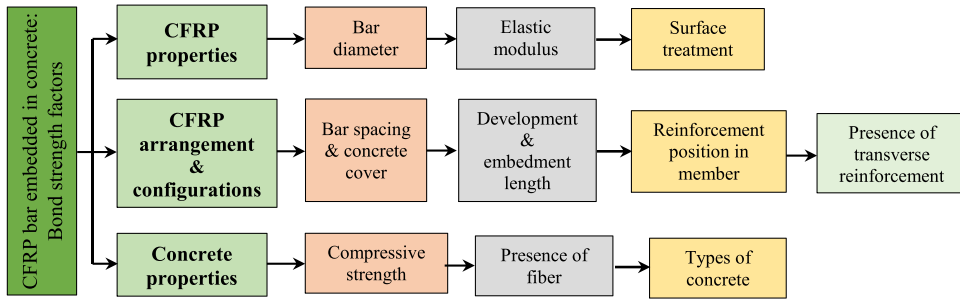
Fig. 2. Parameters affecting bond strength on CFRP bar embedded in concrete [26,27,29,32,36,56,57].

2. Pullout test

ACI 440.3R-12 [58], CSA S806–12 [44] and BS EN 10080:2005 [59] highlight in details on the pullout test to ascertain the bond strength between concrete and CFRP bars. Nevertheless, other methods include beam-end test, simple beam test, hinged beam-end test, splice test and cantilever beam test are recognized as alternative methods to determine the bond strength. However, pullout test has been widely adapted method used to assess the bond strength of embedded CFRP bars in concrete [37–39,60]. For this reason, pullout tests have offered an economical, simplicity and ease of application in performing the test [39,60]. Apart from that, pullout test allows for slip measurement at the unloaded end [48]. Also, limited number of investigations had been conducted on the alternative methods and therefore, experimental database is inadequate for the comparison purposes. Fig. 3 and Fig. 4 show the configuration of conventional and modified pullout test set up in the laboratory, respectively.

2.1. Specimen preparations

CFRP bars should be cut into 1200 mm long section [23]. Nevertheless, in some particular cases, the length of CFRP bars was cut in between 600 mm and 850 mm, so that it can be properly fitted into the testing machine [63–67]. An anchor should be installed at one end of CFRP bar [58]. The anchor should be capable to transmit the loads until failure either by bond failure or concrete splitting [44]. Moreover, the anchor should protect CFRP bars from any damage during the test. Anchorage assembling technique should be in accordance with ASTM D7205/D7205M [68].

The concrete should be designed as a standard mix [44,58]. The concrete cube size may be taken as 200 mm [58] or 150 mm [44] as depicted in Fig. 5. The CFRP bars were vertically embedded with an anchorage length set to be five times of nominal bar diameter [44,58]. The rest of the bar's section should be protected with PVC pipe or any other suitable material to avoid direct contact with the concrete and hence, to prevent bonding. The concrete cube then should be properly compacted by using 16 mm diameter tamping rod [44,58] or vibrating table. The specimens should be properly cured in a curing chamber at 19 °C to 21 °C with relative humidity about 95% until the test day, or a minimum age of 28 days, right after completing the casting works for at least 20 h [44,58]. The curing
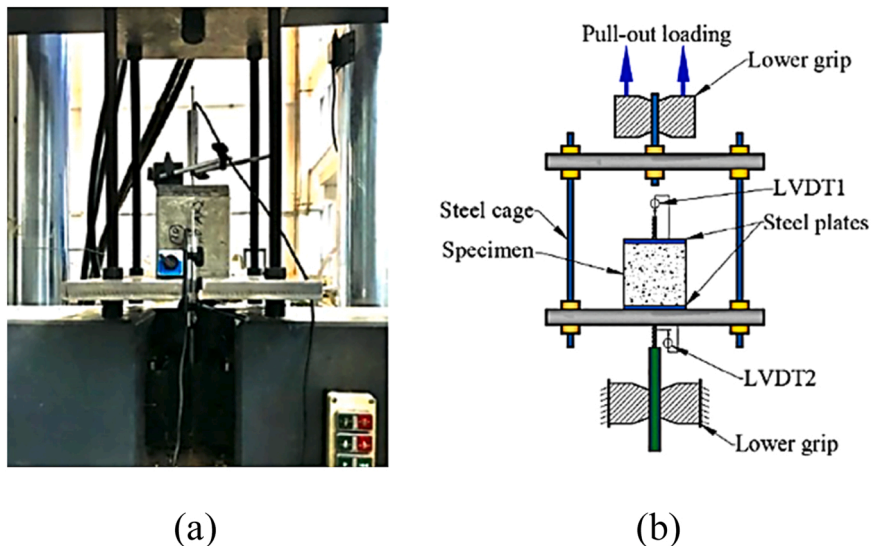

(a) (b)

Fig. 3. Configuration of conventional pullout test [61]: (a) Real test set up; (b) Schematic view.
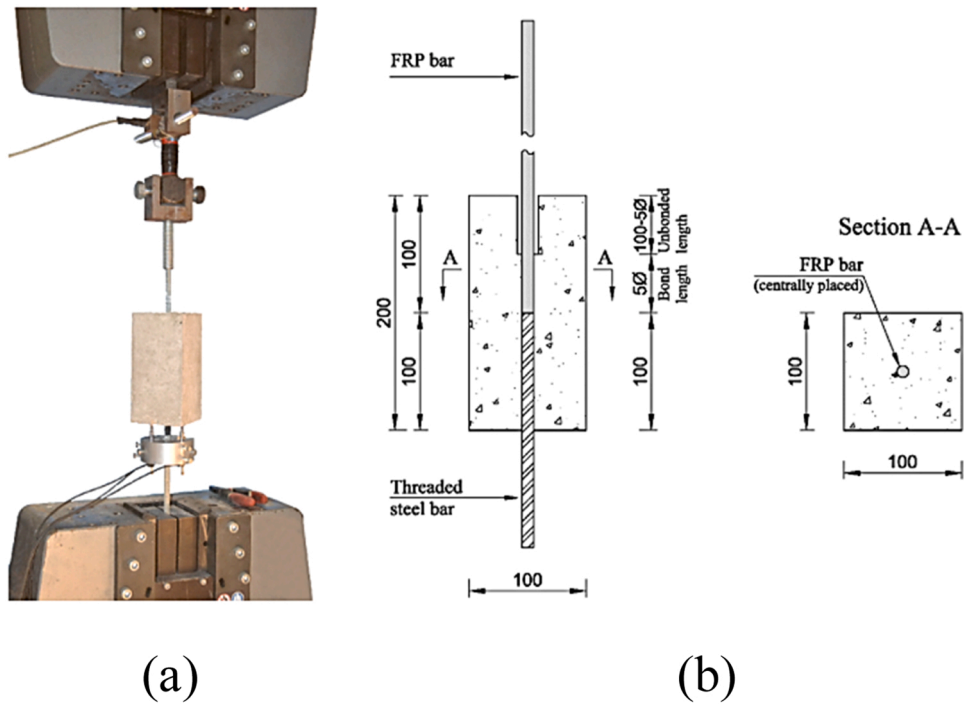
Fig. 4. Configuration of direct tension (modified) pullout test [62]: (a) Real test set up; (b) Schematic representation (all dimensions are in mm).
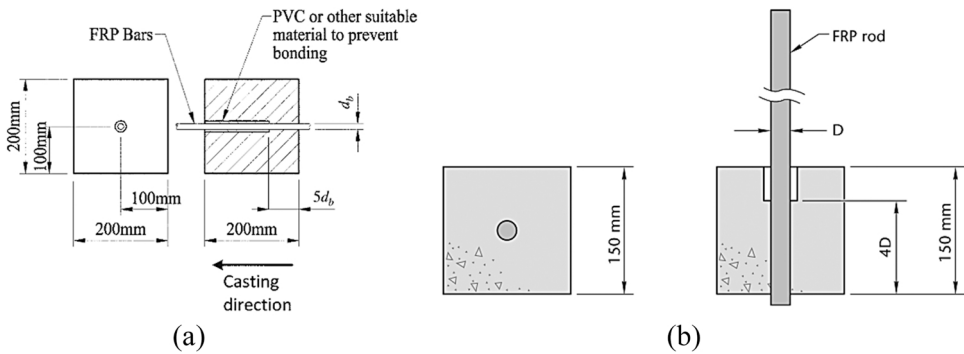

Fig. 5. Specimen preparations for pullout test: (a) 200 mm of concrete cube [58]; (b) 150 mm of concrete cube [44].

process should be in accordance with ASTM C192/C192M [69] or ASTM C511 [70]. One set of pullout test should be represented by five specimens. If any specimen slips at the anchorage section or splits at the concrete cover, an additional test should be executed. The supplemental specimen should come from the same batch as the failed specimen [44,58].

2.2. Experimental procedures

The pullout force should be applied gradually until the bond failure occurs. The test was performed on a universal testing machine (UTM) having maximum capability of 1500 kN. The load rate was not greater than 20 kN/min [58] or 22 kN/min [44] whilst, 1.3 mm/min [58] or 1.27 mm/min [44] for displacement-rate control. Corresponding bar slips were measured using four linear variable differential transformers (LVDTs). Three LVDTs were attached to the loaded end plus another one to the bar's unloaded end [58]. To capture the data transmitted by LVDTs, an automatic data acquisition system was engaged. Throughout the test, the maximum pullout load was set to determine the specimen failure. Also, maximum bond stress and slip values that corresponded to specimen failure were recorded. The test will be ended when the load descents to about 85% of the maximum pullout load or when the slip at loaded end exceeds 8 mm [39]. The pull-out tests should have adhered to ACI 440.3R-12 [58] or CSA S806–12 [44]. Fig. 6 depicts the graphic details of the pullout test setup.

In general, bond strength values are defined as maximum average stress, where maximum pullout load is divided by contact surface
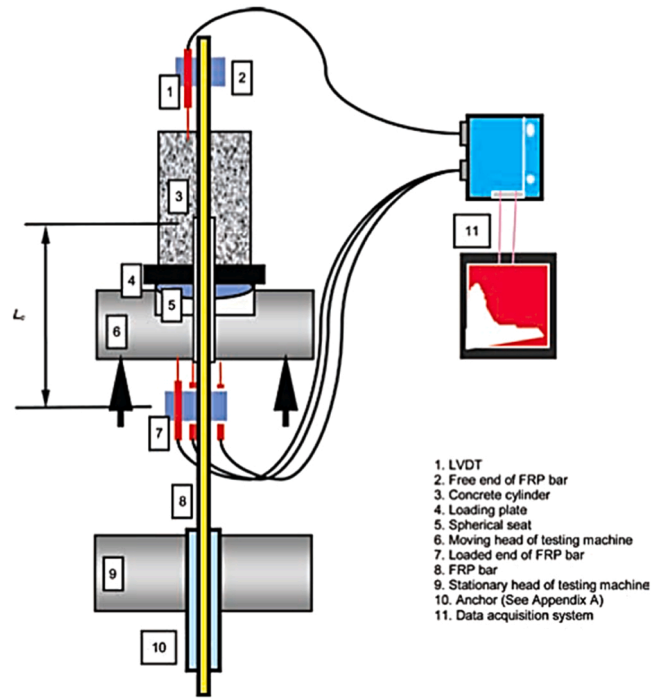
Fig. 6. Graphic details of the pullout test setup [58].

between the concrete and CFRP bar [71]. Hence, bond strength can be calculated by using Eq. (1):

$$\tau = \frac{F}{\pi d_b l_e} \tag{1}$$

In which, τ represents the bond stress (MPa); F is the pullout load (N); d_b is the CFRP bar's diameter (mm); and l_e is the CFRP bar's bonded length (mm).

In pullout test, the corresponding slips recorded at loaded end not only represent the bar slip, but also the bar elongation. Therefore, in order to plot bond stress against slip relationship, the actual bar slip must be determined. Hence, the slip at loaded end (S_{LE}) can be computed by the following equation [72]:

$$S_{LE} = [(S_{LE_{LVDT}-1} + S_{LE_{LVDT}-2} + S_{LE_{LVDT}-3})/3] - S_c \tag{2}$$

where, $S_{LE\ LVDT-1}$, $S_{LE\ LVDT-2}$ and $S_{LE\ LVDT-3}$ are the corresponding slips at loaded end (mm) recorded from LVDT 1, 2 and 3's; and, S_C is the bar's elastic elongation starting from the point where measuring device is installed to the bar's anchorage zone in the concrete. S_C can be determined by using Eq. 2a:

$$S_c = \frac{F L_c}{E_L A} \tag{2a}$$

where, L_c is the length starting from the point where measuring device is installed to the bar's anchorage zone in the concrete (mm); E_L is the bar's elastic modulus (MPa); and A is the area of the bar cross-section (mm^2).

3. Bond stress-slip constitutive model

Mechanisms for transferring the bond stress of embedded concrete with CFRP bars are governed by three significant components: a) mechanical interactions due to irregularity of the CFRP bar surface (deformed bar); b) chemical adhesion between concrete and CFRP bar; and, c) frictional resistance at the interface [48,57,64,71,73,74]. According to the report by Solyom & Balázs [62] and Baena et al. [75], the contribution of these three components may varies subject to the surface condition of CFRP bars. For instance, mechanical interactions are limited only to deformed CFRP bar and primarily responsible in the ascending stage prior to the bond failure. On the other hand, chemical adhesion and frictional resistance play their major roles for non-deformed CFRP bar [76]. Hence, the development of an analytical bond stress-slip model is paramount to present the concrete and CFRP bar's interaction behavior. Moreover, bond stress-slip constitutive law is required to conduct numerical analysis and predict maximum bond strength. The developed bond stress-slip models are briefly revised in the following section.

3.1. Malvar model

Malvar [42] had conducted an extensive investigations on four different surface textures of glass FRP (GFRP) bars. Malvar [42] has proposed a polynomial function to calculate the bond strength. This function is relying on the two curve fitting parameters of F and G. The following equation illustrates this model.

$$\tau = \tau_m \frac{F\left(\frac{s}{s_m}\right) - (G-1)\left(\frac{s}{s_m}\right)^2}{1 + (F-2)\frac{s}{s_m} + G\left(\frac{s}{s_m}\right)^2} \tag{3}$$

where, τ_m and s_m are the maximum bond stress (MPa) with its slip (mm), respectively; s is the corresponding slip (mm) with respect to the bond stress; and, F and G are the curve fitting parameters for different types of bar. In addition, to estimate τ_m and s_m with determined value of confinement pressure, σ_r, Malvar [42] has proposed other two relationships as follows:

$$\frac{\tau_m}{f_t} = A + B\left(1 - e^{-C\sigma_r/f_t}\right) \tag{3a}$$

$$s_m = D + E\sigma_r \tag{3b}$$

where, σ_r is confining axisymmetric radial pressure (MPa); f_t is the tensile strength for concrete (MPa); and, A, B, C, D, E are the curve fitting parameters determined for different types of bar. It can be observed from this model that a significant number of empirical constants, such as A, B, C, D, E, F, and G are required to be ascertained first. Hence, bond stress-slip behavior cannot be accurately predicted from the equations unless an extensive investigations have been done for the various type of FRP bars [47].

3.2. BPE and modified BPE model

The well-known BPE (Bertero, Popov and Eligehausen) model was suggested by Eligehausen et al. [41] for deformed steel bar as depicted in Fig. 7a. This analytical model later on was slightly modified by Cosenza et al. [71] as shown in Fig. 7b. The comparison between of these two models, Cosenza et al. [71] had considered the absentee of plateau as steel bar, in FRP bond behavior. The modified BPE model was principally separated into three stages. The first stage represents the ascending pattern of bond behavior, which corresponds to the mechanical interlock and chemical adhesion. In stage 2, FRP bar begins to slip after the bond stress has attained its maximum capacity. The bond strength in stage 1 starts to diminish and resulting rapid increase in slip. Cracks at the interface (or even concrete crushing) might be developed as well in this softening stage. Finally, significant failure appears including bar pullout or concrete cracks in stage 3. The FRP bar continues to slide and the horizontal branch indicates the friction component between FRP bar and concrete [71]. These 3 stages can be expressed by analytical law in the equations below:

$$\frac{\tau}{\tau_m} = \left(\frac{s}{s_m}\right)^\alpha \quad \text{for} \, 0 \le s \le s_m \tag{4a}$$

$$\frac{\tau}{\tau_m} = 1 - p\left(\frac{s}{s_m}\right) \quad \text{for} \, s_m \le s \le s_2 \tag{4b}$$

$$\tau = \tau_r \quad \text{for} \, s \ge s_2 \tag{4c}$$

where, α and p are the curve fitting parameters from experimental results. It is noteworthy that this model takes the impact of surface condition on bond behavior into account. However, neither the type of fibre used nor the bar's diameter were investigated by this model.
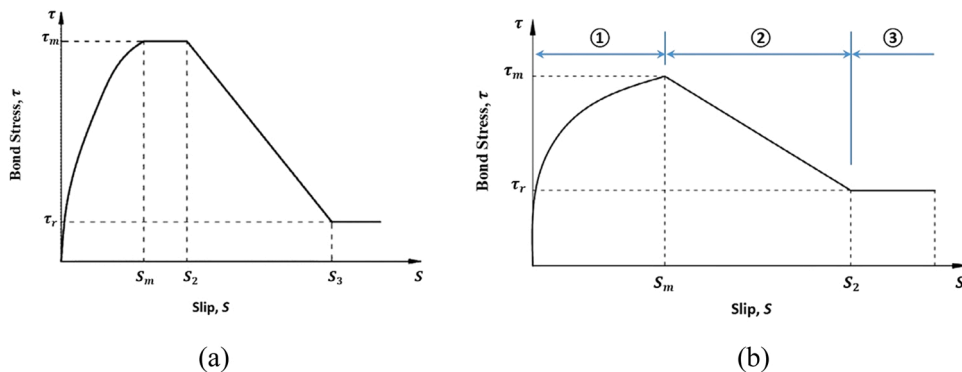

Fig. 7. Bond stress-slip model: (a) BPE model [41]; and, (b) Modified BPE model [71].

3.3. CMR model

The CMR (Cosenza, Manfredi and Realfonzo) model [77] refine the bond stress-slip curve by considering only the ascending stage (i.e. pre-peak bond behavior). This consideration was taken due to the circumstances where most structural design issues are resolved at the serviceability limit state. The ascending function is defined by the following expression:

$$\frac{\tau}{\tau_m} = \left(1 - e^{\left(-\frac{s}{s_r} \right)} \right)^{\beta} \tag{5}$$

where, s_r and β are the curve fitting parameters from experimental results. It can be noticed that the initial slope provide by CMR model is equal to infinity. This indicate that the effect of chemical adhesion are taking into account at the initial stage [71].

3.4. Tighiouart et al. Model

Another model was developed by Tighiouart et al. [78] as replacement curve for the ascending stage. They had calibrated the parameters of s_r and β in the CMR model. The function of ascending stage is expressed by the equation below.

$$\frac{\tau}{\tau_m} = \left(1 - e^{(4s)} \right)^{0.5} \tag{6}$$

It can be evaluated the proposed model is dependent on the peak bond stress, as shown by Eq. 6. Nevertheless, Tighiouart et al. [78] had manifested that several factors may affect this peak bond stress. Those factors include bar surface profile, bar diameter and embedment length. Hence, to incorporate this function into the numerical analysis, the peak bond stress data based on the various cases must be documented. Also, it is noteworthy that Tighiouart et al. model [78] only consider the ascending stage where it is suitable for the analysis at serviceability state level, same observation on the CMR model [71].

3.5. Comparison of bond stress-slip constitutive model

Table 1 summarized on these four bond stress-slip model for their merits and drawbacks in predicting the bond behavior. It should be noted that certain assumptions and factors were taken into consideration when developing and deriving the existing bond stress-slip models. It is clear that surface treatment and GFRP bars were the common variables considered in their investigations. As compared to the others, Malvar model was less reliable and less accurate [45,79]. One of the reasons is that Malvar model requires seven empirical constants, which must be determined by curve fitting from experimental studies. The values for these constants are listed in Table 2. Moreover, the value for σ_r is difficult to be calculated for the structures that are subject to bending loads [79]. The ignorance on the impacts of bar diameter and fiber type could contribute the drawback factors for this model.

Differently, modified BPE and CMR models requires only two curve fitting parameters need to be determined. On the hand, Tighiouart et al. model requires no empirical constant in their proposed ascending function. By comparing these three models, Modified BPE model offers an entire bond stress-slip curve which include pre and post-peak bond behavior for CFRP bars. Meanwhile, CMR and Tighiouart et al. models consider only the ascending stage as it is suitable for the analysis at serviceability state level. Based on Masmoudi's work [80], Modified BPE model over-estimates the ascending stage as compared to the experimental values but was

Table 1
Comparison of bond stress-slip models.

Evaluation aspect	Malvar model[42]	Modified BPE model[71]	CMR model[77]	Tighiouart et al. Model[78]
Parameters investigated	a) Confinement; and, b) Surface treatment (indention depth).	Surface treatment	a) Fiber types b) Surface treatment	a) Surface treatment b) Diameter c) Embedment length
Type of fiber considered	E-glass	a) Carbon; b) Glass; and, c) Aramid	a) Carbon; b) E-glass c) Glass; and, d) Aramid	Glass
Bond stress-slip curve equation	Polynomial function	Three piecewise equations (for three-stages)	One piecewise equation (for ascending stage)	One piecewise equation (for ascending stage)
Curve fitting value from experimental works (refer to Table 2)	Seven parameters (e.g.: A, B, C, D, E, F and G)	Two parameters (e.g.: α and p)	Two parameters (e.g.: s_r and β)	None
Reliability	a) Less reliable in the ascending stage; b) Value for σ_r is difficult to be calculated for structures that are subject to bending loads; and, c) Impacts of bar diameter and fiber type were not considered.	a) Present an entire bond stress-slip curve (pre and post-peak bond behavior); and, b) Ascending stage over-estimate the experimental values.	a) Presents only the ascending curve (pre-peak bond behavior); b) Inadequate for a complete analysis of structures till failure; and, c) Good performance with experimental results.	a) Presents only the ascending curve (pre-peak bond behavior); b) Insufficient for a comprehensive structural analysis until failure.

Table 2
Parameters for defining bond stress-slip models.

Surface treatment	Malvar model[42]						
	A	B	C	D	E	F	G
Indented (Type A)	1.00	0.94	0.05	0.0202	5.87E-6	11.0	1.2
Indented (Type D)	0.266	5.63	0.15	0.0475	5.23E-5	13.0	0.5
Surface treatment	**Modified BPE model[71]**						
	α	p	s_m	τ_m	τ_r		
Smooth	0.145	1.87	0.26 mm	1.19 MPa	0.99 MPa		
Grain covered	0.067	3.11	0.13 mm	12.05 MPa	3.17 MPa		
Sandblasted	0.251	2.63	1.08 mm	2.74 MPa	1.38 MPa		
Twisted	0.175	4.15	0.45 mm	4.15 MPa	3.68 MPa		
Ribbed	0.283	14.88	1.23 mm	11.61 MPa	7.79 Mpa		
Indented & braided	0.177	12.80	2.14 mm	10.20 MPa	6.26 MPa		
Braided & sanded	0.069	0.95	0.15 mm	17.78 MPa	7.13 MPa		
Surface treatment	**CMR model[77]**						
	s_r	β	τ_m				
Smooth	0.11 mm	0.314	1.19 MPa				
Grain covered	0.07 mm	0.138	12.05 MPa				
Sandblasted	0.41 mm	0.559	2.74 MPa				
Twisted	0.12 mm	0.593	4.15 MPa				
Ribbed	0.45 mm	0.575	11.61 MPa				
Indented & braided	0.78 mm	0.473	10.20 MPa				
Braided & sanded	0.08 mm	0.025	17.78 MPa				
Spirally wounded	3.33 mm	0.260	13.14 MPa				

assessed as being more precise than Malvar Model. They have also manifested that CMR model had shown an excellent results with experimental findings and most suitable in modelling the ascending stage [80,81]. However, the absentee of post-peak behavior in CMR and Tighiouart et al. models make it less intention to be used in numerical analysis. Moreover, the ascending function proposed by Tighiouart et al. [78] was claimed to have an error due to the value of corresponding slip, *s* that mathematically determined to be a negative value [79].

Based on the comparisons made above, it appears the modified BPE model is the most proper and practical model as it offers a complete bond stress-slip curve for embedded CFRP bars in concrete. Nevertheless, with the ascending stage of CMR model is capable to present the most precise pre-peak bond stress-slip behavior, it has attracted great interest of using CMR model as a replacement for the ascending stage of modified BPE model to assess the entire bond stress-slip performance for CFRP bars [79].

4. Bond strength predictions by international design provisions

4.1. ACI committee 440 (ACI 440.1R-15)

According to ACI 440.1R-15 [23], the normalized bond strength ($\frac{\tau}{\sqrt{f_c'}}$) is linearly regressed against the normalized concrete cover ($\frac{C}{d_b}$) and normalized splice length ($\frac{d_b}{l_e}$). The expression in Eq. 7 used to determine the bond strength:

$$\frac{\tau}{0.083\sqrt{f_c'}} = 4.0 + 0.3\frac{C}{d_b} + 100\frac{d_b}{l_e} \tag{7}$$

where, f_c' is concrete compressive strength (MPa) at 28-days; and, *C* is the distance either the cover to the center of the bar or one-half of the center-to-center spacing of the bars that being developed (mm), whichever is lesser. Eq. 7 was developed with regard to the extensive study by Wambeke and Shield [82] throughout their database on 269 beams bond strength test. The database comprehensively covered GFRP bars that were being tested in beam-end tests, notch-beam tests and splice tests. Sand coated (SC), spiral wrap and helical lug, with and without confining reinforcements were among the different variables in surface condition. The bar had diameter in the range of 13–29 mm embedded in 28–45 MPa of concrete strength. From a total of 240 GFRP samples, the experimental results had manifested that 75, 94 and 71 specimens had failed due to concrete splitting, pullout failure as well as bar tensile fracture, respectively. They also observed that bar surface treatment did not seem to give an impact on the test results.

4.2. Canadian standards association (CSA S806-12)

According to the CSA S806–12 [44], Eq. 8 is proposed to estimate the average bond strength for concrete embedded with CFRP bars:

$$\tau = \frac{d_{cs}\sqrt{f_c'}}{1.15(K_1K_2K_3K_4K_5)\pi d_b} \tag{8}$$

where, the value for d_{cs} is the shortest distance between the center of developing bar to the nearest concrete surface or two-thirds of the center-to-center spacing between developing bars (mm); K_1 is defined as a factor for bar location (1.3 for horizontal reinforcement placed so that more than 300 mm of concrete thickness is cast below the bar; 1.0 in all other situations); K_2 is defined as a factor for concrete density (1.3 for structural low-density concrete; 1.2 for structural semi-low-density concrete; 1.0 for normal density concrete); K_3 is defined as a factor for bar size (0.8 for $A_b \leq 300$ mm^2 equivalent to bar diameter ≤ 9.78 mm; 1.0 for $A_b > 300$ mm^2 equivalent to bar diameter > 9.77 mm); K_4 is defined as a factor for types of fiber (1.0 for CFRP bar); K_5 is defined as a factor for bar surface condition (1.0 for surface-roughened or SC or braided surfaces; 1.05 for spiral pattern or ribbed surfaces; 1.8 for indented surfaces;). If the bar surface condition factor has been demonstrated through tests, the K_5 factor may be taken as less than 1.0 but not less than 0.5. Also, bond test should be conducted to determine the K_5 factor for additional type of surface condition or combinations of surface profiles. Hence, it can be noted that Eq. 8 is not considering the functions of embedment length and transverse reinforcement to calculate the bond strength.

4.3. Canadian highway bridge design code (CSA S6-06) and ISIS Canada

Alternative international design guidelines are CSA S6–06 [83] and ISIS Canada [24] have specified that the bond strength for concrete embedded with CFRP bars can be determined by the following equation:

$$\tau = \frac{f_{cr}(d_{cs} + K_{tr}E_{FRP}/E_s)}{0.45\pi d_b K_1 K_4} \tag{9}$$

where, f_{cr} is the value for concrete cracking strength (MPa); K_{tr} is the transverse bars index and can be defined in Eq. 9a; E_{FRP} is elastic modulus for CFRP bar (MPa); E_s is elastic modulus for steel bar (MPa); K_1 is defined as a factor for bar location; K_4 is defined as a factor for bar surface condition (not greater than 1.0 to represent the bond strength ratio for CFRP to steel bar having the same diameter or 0.8 for the absence of product data).

$$K_{tr} = \frac{A_{tr}f_y}{10.5sn} \tag{9a}$$

where, A_{tr} is transverse bars area perpendicular to the split plane through the bars (mm^2); f_y denotes the transverse bars yield strength (MPa); s is the transverse bars center-to-center spacing (mm); n is the number of bars along the split plane. Therefore, it can be evaluated from Eq. 9 that only the embedment length factor is not considered by CSA S6–06 [83] and ISIS Canada-2007 [24] in predicting the bond strength.

4.4. Japanese design code (JSCE)

JSCE [84] proposes a relationship in calculating the bond strength as specified in Eq. 10:

$$\tau = f_{bod}/\alpha_1 \tag{10}$$

where, f_{bod} denotes as designed concrete's bond strength (MPa) and can be defined by Eq. 10a; α_1 stand as confinement modification factor and can be calculated with Eq. 10b as follows.

$$f_{bod} = \frac{0.28\alpha_2 f_c'^{\frac{2}{3}}}{1.3} \leq 3.2N/mm^2 \tag{10a}$$

$\alpha_1 = 1.0\, for\, k_c \leq 1.0;$

$\alpha_1 = 0.9\, for\, 1.0 < k_c \leq 1.5;$

$\alpha_1 = 0.8\, for\, 1.5 < k_c \leq 2.0;$ $\tag{10b}$

$\alpha_1 = 0.7\, for\, 2.0 < k_c \leq 2.5;$

$\alpha_1 = 0.6\, for\, k_c > 2.5;$

α_2 denotes the bond strength modification factor (value of 1.0 should be applied if the bond strength is equal or greater than deformed steel bars or else, value shall be adjusted pertaining to experimental data); and, k_c can be determined from Eq. (10c) below.

$$k_c = \frac{C}{d_b} + \frac{15A_t}{sd_b}\frac{E_t}{E_s} \tag{10c}$$

where C is the shortest distance between the bottom reinforcement concrete cover or half of the distance between developed reinforcement (mm); A_t is the area for transverse bars (mm^2); s is the spacing for transverse bars (mm); E_t is the elastic modulus for transverse bars (MPa); and, E_s is the elastic modulus for steel bar (MPa). It can be noticed from Eq. 10 that JSCE [84] has neglected the

factors like embedment length, bar surface condition fiber type in calculating the bond strength.

4.5. Comparison of predicted bond strength on CFRP bars

Table 3 provides the main factors that influence the bond strength prediction as proposed by international design guidelines. Apart from that, comparative study between the predicted values for bond strength by international design guidelines against the experimental results of bond strength is shown in Fig. 8. Additionally, selected statistical measures include the performance factor (PF), coefficient of variation (COV), the average absolute error (AAE) and root mean squared error (RMSE) were conducted to evaluate the performance of these international guidelines in predicting bond strength [57,85,86]. The results on statistical measure are summarized in Table 4. It is evident that ACI 440.1R-15 [23] and JSCE [84] underestimate the bond strength. As opposed to that, CSA S806–12 [44] and CSA S6–06 [83] & ISIS Canada [24] overestimate the bond strength by 20% and 24%, respectively. This can be explained by the numerous factors considered by CSA S806–12 [44] and CSA S6–06 [83] & ISIS Canada [24] in predicting the bond strength by referring to the Table 3.

It is interesting to note from Fig. 8 that there have no relationship at all between the predicted bond strength by international design guidelines against the experimental results. Nonetheless, statistical measures have indicated that all international design guidelines are having COV in the range of 46.20% and 62.44%. This percentage shows that high dispersion between predicting the bond strength and experimental ones. Furthermore, the international design guidelines have also recorded high percentage in AAE between 80.09% and 175.09%. In addition to that, ACI 440.1R-15 [23] has the lowest RMSE value of 7.95 whilst, JSCE [84] are the highest with RMSE value of 12.13. These AAE and RMSE values indicate the amount of error and accuracy in predicting the bond strength. These observations are in line with the reports from the existing literatures that predicting values of bond strength by international guidelines are conservative [45,57,72,87]. The variations of parameters considered as listed in Table 3 have contribute to these observations, giving good fits in some cases and large differences in others. Nevertheless, throughout the statistical measures, bond strength prediction by ACI 440.1R-15 [23] is discovered to be more realistic as compared to the experimental results.

5. Characteristic bond behavior between CFRP bar and concrete

5.1. Variation in concrete compressive strength

5.1.1. Failure mode

Fig. 9 shows the relationship between types of failure mode associated with concrete compressive strength. The experimental data had shown that bar pullout failure were dominant for all categorized of concrete compressive strength, accounted about 73% from all specimens. Specifically, concrete splitting failure and bar rupture were only observed in the compressive strength range of 20–60 MPa. Besides, peeling off resin was observed from 20 MPa and above. Also, in terms of compressive strength as the variables, preceding researchers by Achillides & Pilakoutas [39] had manifested that concrete shear strength was controlling the failure mode particularly for low compressive strength around 15 MPa. They had discovered that the concrete crushed between the bar deformations. However, for higher concrete strength about 30 MPa, the bond failure appeared to be dominated by the interlaminar shear strength of CFRP bar rather than just concrete strength. They had discovered the failure may have occurred partially on the bar surface or concrete crushed [39]. Nonetheless, for concrete strength even higher than 50 MPa, Baena et al. [75] and Solyom & Balázs [62] had demonstrated the surface damage to CFRP bar during bond failure. They had found that the ratio of delaminated surfaces in CFRP bars with SC layer is greater, as shown in Fig. 10. In addition to that, Fig. 11 shows the bar's pullout failure for deformed bars with damages and deeper scratches, as well as in particular cases, had partial shearing off the lug or rib deformation. Therefore, the integrity for deformed bars with damages and deeper scratches seems to be controlled by critical interface shear strength between resin and the fibers itself. As a result, it is evident that the increment of compressive strength will consequence in more damage to the CFRP surface during the bond failure.

5.1.2. Bond strength

As verified by preceding researchers, a strong correlation had been reported between bond strength and the square root of compressive strength [39,66,95]. Thus, Fig. 12 is plotted to observe the relationship between of these two components. It can be clearly observed that heavy data for pull-out test were tested at the range of 25 MPa and 70 MPa. General observation can be made from the graph that increasing the concrete compressive strength resulting in increment of bond strength, same as reported in the existing

Table 3
Factors considered to calculate bond strength according to international guidelines.

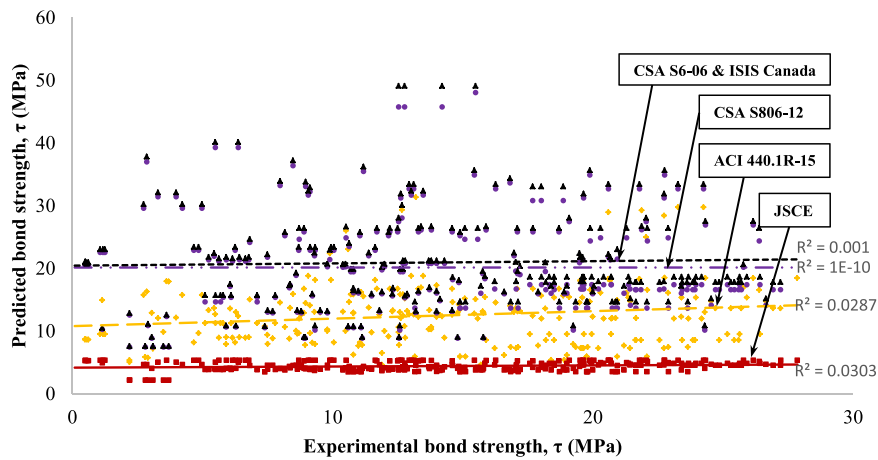| Design guidelines	Concrete strength	Bar diameter	Concrete cover	Bar location	Embedded length	Bar surface	Transverse confinement	Fiber type
ACI 440.1R-15[23]	✓	✓	✓	✓	✓	X	X	X
CSA S806–12[44]	✓	✓	✓	✓	X	✓	X	✓
CSA S6–06[83] & ISIS Canada[24]	✓	✓	✓	✓	X	✓	✓	✓
JSCE[84]	✓	✓	✓	✓	X	X	✓	X

Fig. 8. Comparison on the prediction values for bond strength by international design guidelines against the experimental results of bond strength [29,38,39,48,61,63–66,72,75,76,88–94].

Table 4
Statistical measures on bond strength by international guidelines.

Design guidelines	Avg. PF	COV (%)	AAE (%)	RMSE
ACI 440.1R-15[23]	1.30	62.44	86.90	7.95
CSA S806–12[44]	0.80	56.50	170.46	11.62
CSA S6–06[83] & ISIS Canada[24]	0.76	55.09	175.09	12.01
JSCE[84]	3.30	46.20	80.09	12.13
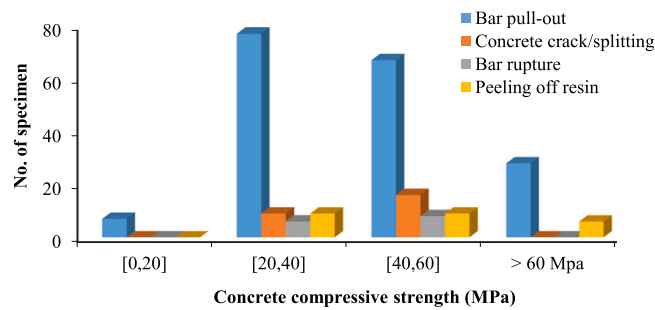
Fig. 9. Relationship between types of failure mode associated with concrete compressive strength [29,38,39,48,61,63–66,72,75,76,88–94].
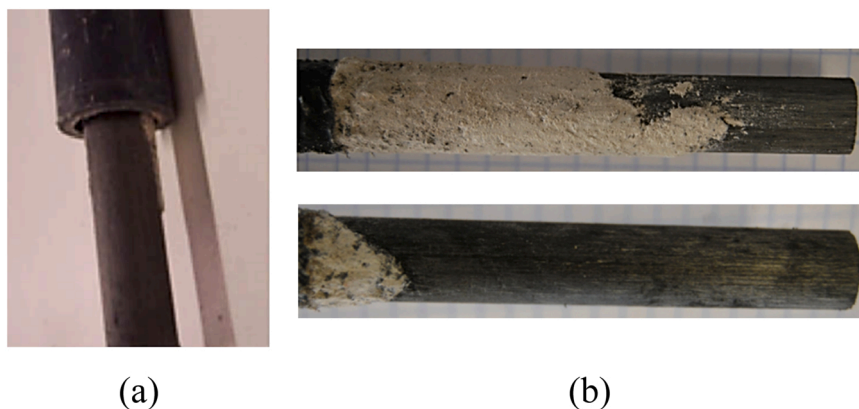
Fig. 10. Bond failure surface of CFRP bar with SC: (a) peel off of the whole SC layer [75]; (b) peel off the part of SC layer [72].
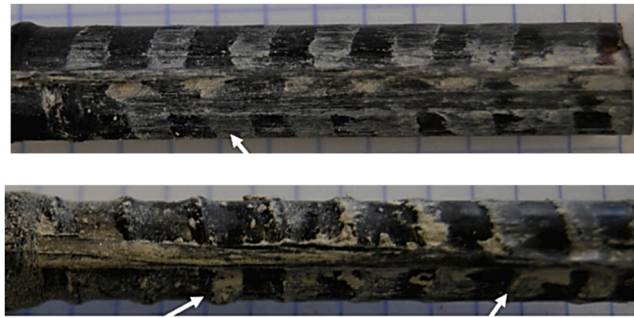
Fig. 11. Ribbed CFRP bar pull-out failure with shearing off the rib [72].
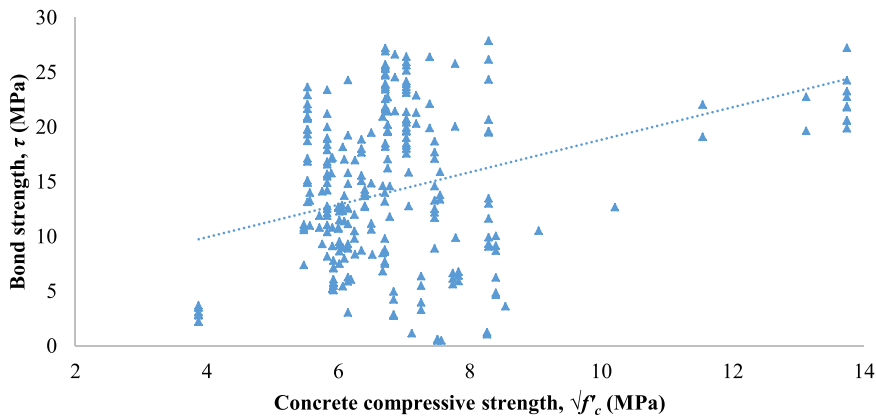

Fig. 12. Implication of concrete compressive strength to the bond strength of CFRP bar [29,38,39,48,61,63–66,72,75,76,88–94].

literatures [40,62,75,96,97]. The perfect combination between high strength concrete with CFRP bar resulted a significant increment of radial stress surrounding the CFRP bar. Moreover, improving of material characteristics and surface treatment on CFRP bars might as well contribute to this result. As reported by Caro et al. [63], by increasing the compressive strength from 26 MPa to 46 MPa, average bond strength were increased by 33%. Another investigations by Zhao et al. [94] and Achillides & Pilakoutas [39] have observed the same pattern with the increment of bond strength for 63% and 124% by increasing the compressive strength from 36 MPa to 60 MPa and 15–46 MPa, respectively.

In terms of bond strength predictions, Pour et al. [57] had summarized the important effect of concrete compressive strength. They had highlighted that ACI 440.1R-15 [23] and CSA S806–12 [44] codes were capable to estimate the bond strength that only related to the concrete with normal strength. However, for high strength concrete which is greater than 50 MPa, bond strength predictions by ACI 440.1R-15 [23] and CSA S806–12 [44] were more conservative.
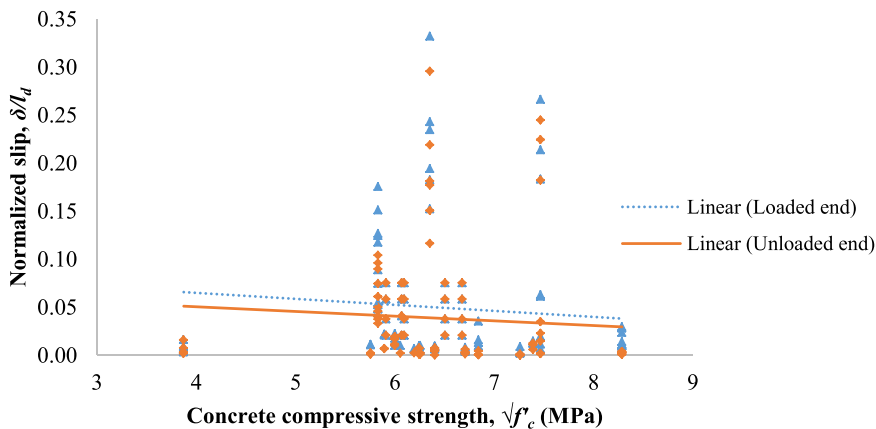

Fig. 13. Impact of compressive strength on the normalized slip [29,38,39,48,61,63–66,72,75,76,88–94].

5.1.3. Corresponding slip

Data from the literatures have been analyzed to observe the corresponding slip against concrete strength. Fig. 13 illustrates the scattered data on the impact of being increased on concrete compressive strength to the normalized slip. The y-axis in Fig. 13 represents the normalized slip, δ/l_d where, it is a ratio of the corresponding slip, δ to the embedded length of CFRP bars in concrete, l_d. Experimental data have pointed out that slip at the loaded end were higher than that at the free end. Also, it can be noticed from the graph that the overall normalized slip is decreasing with the increment in compressive strength. In a study by Caro et al. [63], they have also recorded about 40% decreased for normalized slip at loaded end with the increment in compressive strength, the same agreement was reported by existing literatures [48,72,76]. In line with this statement, Fig. 13 has shown that the overall statistical measure indicates the normalized slip is descending (for both loaded and unloaded end) particularly for the concrete compressive strength over than 40 MPa. This results demonstrate that the relative bond stress moves progressively from the loaded end to the free end with lower slippage at relative high strength concrete [45]. As the pullout load increased towards its peak bond strength, it can be suggested that bond had failed by sudden, unexpected and brittle failure caused by the confinement effect of high strength concrete [48].

5.2. Effect of different embedment length

5.2.1. Failure mode

Embedment length, l_d is an another imperative factor dominating the bond strength of embedded concrete with CFRP bars. Fig. 14 is plotted to compare the experimental data on types of failure mode associated with the ratio of embedment length to bar diameter, l_d/d_b. It can be stated that pullout failure governs the failure modes as it was designed for. Additionally, the mean value of a normal distribution between 5 and 10 of l_d/d_b is produced by the column chart. This embedment length (5–10 times of bar diameter) represents for over-all of 115 samples had been failed by pulling out. It can be suggested that embedment length between 5 and 10 times of bar diameter can provide the desired bond pullout failure. According to the preceding investigation on the increment of embedment length, multiple of ribs delaminated from the bar's core had been discovered on ribbed CFRP bars throughout the pullout failure [37, 38,88,94], as depicted earlier in Fig. 11. Same observation was recorded on CFRP bar with SC, presented in Fig. 10 [37,88]. The experimental results have indicated that bond performance of CFRP bars could be influenced by the interlaminar shear strength. Moreover, sufficient embedment length may have resulted in bar tensile failure particularly when l_d/d_b exceeding 15. Fig. 15 exhibits the example of bar tensile failure in pullout test. On the other hand, another type of bond failure is concrete split as shown in Fig. 16. Concrete split occurs by sudden and brittle failure due to the concrete that had failed in tensile. This kind of failure mode induced by a crack that propagate to the central hole and the concrete cube was split into two fragments.

5.2.2. Bond strength

Data mined form literatures were also analysed on the influence of embedment length against bond strength. The relationship related to the normalized bond strength and l_d/d_b ratio for CFRP bars is presented in Fig. 17. The graph demonstrates a general pattern in which the normalized bond strength decreases as l_d/d_b ratio increases. Other researchers who conducted their own investigations observed the same behavior [39,47,57,63,64]. For instance, Achillides et al. [39] concluded in their investigation that a decrease in FRP bar's maximum bond stress is caused by the increment of embedment length. This phenomenon can be interpreted by the nonlinear bond stress distribution at the interface between concrete and CFRP bar [39,98]. Moreover, previous study had manifested that nominal bond strength increases promptly at the interface of shorter embedment length than the longer ones [39,47,65,71]. It can be also noticed that higher pullout load required along with the increment of embedment length. In addition, the initial bond stiffness of CFRP bar is significantly affected by embedment length [39]. The ACI 440.1R-15 [23] in Section 4.1 also supports this conclusion.

5.2.3. Corresponding slip

The database was further studied for valuable information on the normalized slip against l_d/d_b ratio as depicted in Fig. 18. Parametric study demonstrates the ascending pattern for corresponding slip as the embedment length increased, same observation has been discovered in the literatures [48,65,76]. This increasing pattern is related to the nonlinear bond stress distribution throughout the
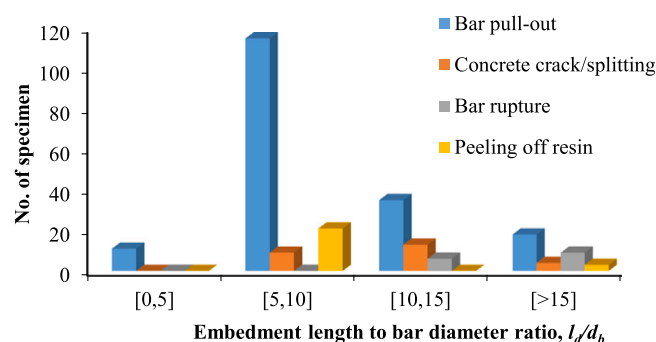

Fig. 14. Comparison on types of failure mode with respect to l_d/d_b ratio [29,38,39,48,61,63–66,72,75,76,88–94].
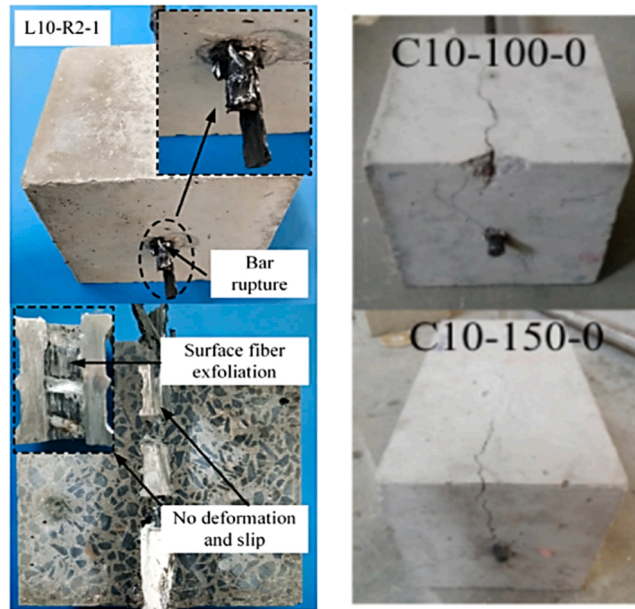
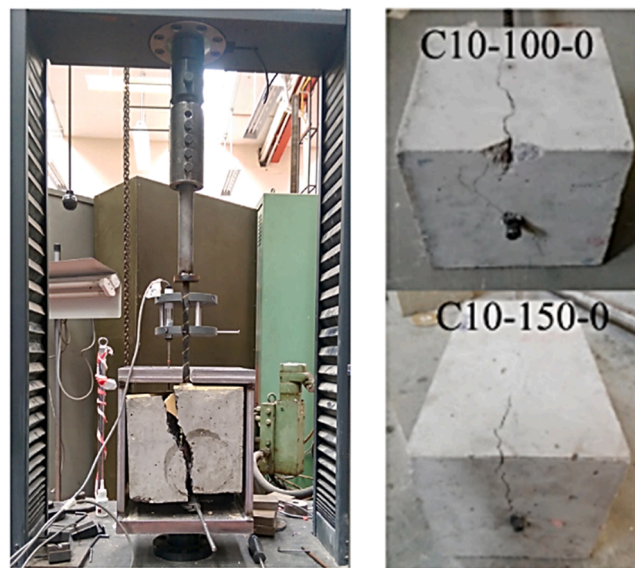**Fig. 15.** CFRP bar rupture failure in pullout test [64,93].

Fig. 16. Concrete splitting failure in pullout test [63,93].

contact area between concrete and CFRP bars [47,48]. In addition to that, the longer embedment length requires higher pullout force upon bond failure. And, the greater embedment length affords an extensive strain length to enhance bar's deformation while being pulled out with higher force. Hence, FRP bars were frequently having bond failure with larger slip.

5.3. Variation in bar diameter

5.3.1. Failure mode

The types of failure mode in relation to bar diameter is presented in Fig. 19. Again, pullout failure overwhelms the failure modes [38,39,48,65,72,75,88,94]. The column chart generally displays the mean value of a normal distribution between 10 and 12 mm diameters, represents for over-all of 79 samples had been failed by pulling out. It indicates that the CFRP bar with 10–12 mm diameter can provide the desired bond pullout failure. It also seems that the highest splitting failures, bar rupture and peeling off resin were
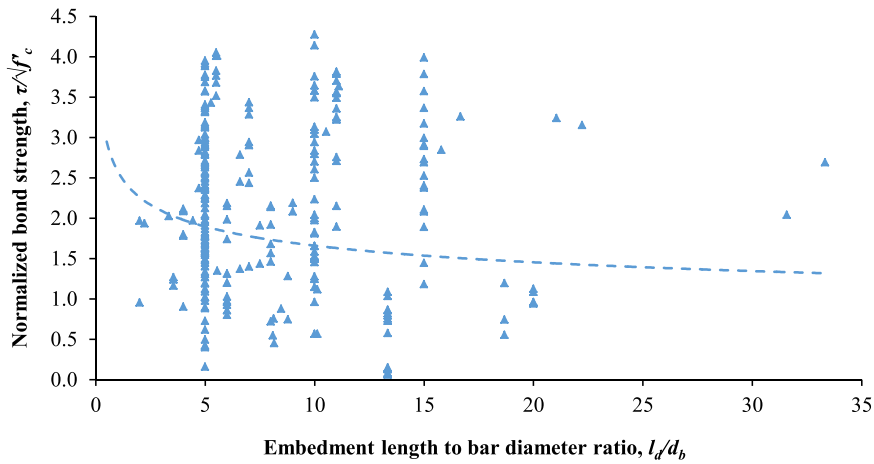
Fig. 17. Relationship on the normalized bond strength against l_d/d_b ratio [29,38,39,48,61,63–66,72,73,75,76,88–94].
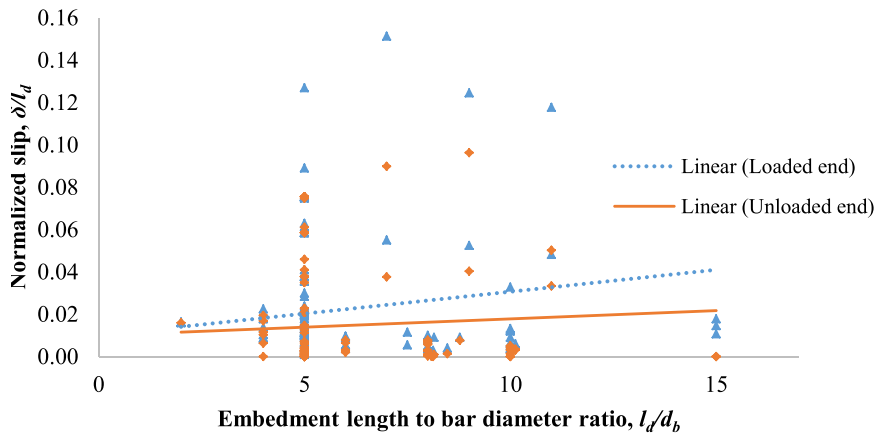

Fig. 18. Relationship on the normalized slip against l_d/d_b ratio [29,38,39,48,61,63–66,72,75,76,88–94].
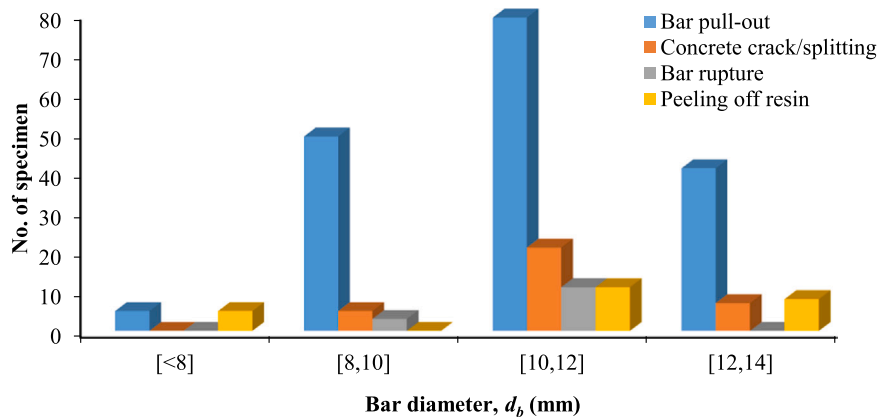

Fig. 19. Type of failure modes distribution against bar diameter [29,38,39,48,61,63–66,72,75,76,88–94].

observed at 10–12 mm diameters with 21 specimens, 11 specimens and 11 specimens, respectively. As far as author concerns, there is limited information on the specific influence on bar diameter to the type of failure modes. Nonetheless, Lee et al. [65] had found that larger bar diameter yields a brittle nature in bond failure due its greater amount of elastic energy. Other than that, bar diameter relatively has more significant impact on bond strength as well as its corresponding slip. A good number of research studies had

suggested several factors that may be considered which include surface contact area, Poisson effect, and shear lag phenomenon [39,48, 65,75].

5.3.2. Bond strength

Fig. 20 presents the scattered data related to bond strength and CFRP bar diameter. The plotted graph indicates that bond strength decreases as the bar diameter increases, agreed with the conclusions reach by the literatures [39,47,48,57,66,71,99]. Also, the international design provisions as discussed in Section 4 lead to the same identical conclusion. Hence, such observation can be accounted by the significant magnitude of elastic energy reserved in greater bar diameters [75], contact area between bar and concrete [48,99], Poisson ratio effect and shear lag phenomenon [24,39,48,100]. In terms of contact area, as the bar diameter increased, it is naturally trap the void underneath the bar caused by the water bleeding in concrete [48]. Consequently, increase the possibility to limits the contact surface between the bars with concrete and, eventually lead to a lower bond strength. In addition to that, according to some authors [39,65], nonlinear stress distribution could clarify the bond strength dependency on bar diameter. Moreover, Poisson ratio effect could have explained the bar diameter's impact on bond strength where CFRP bar experiences in diameter reduction when it pulled under tension [39,48,65]. Loss in frictional resistance and mechanical interaction may result from the diameter reduction. Besides, by comparing to smaller diameter, greater bar diameter requires extended embedment length to generate the same magnitude of bond strength and developed lower adhesion with the surrounding concrete [39].

5.3.3. Corresponding slip

An interaction between bar diameter and its corresponding slip is plotted and presented in Fig. 21. Data from literatures have specified that greater bar diameter results in less slip. The main reason is being caused by the significant magnitude of elastic energy reserved in greater bar diameters [75], greater contact area of the bar with surrounding concrete [99] and shear lag phenomenon [24, 39,48,100]. Fig. 22 illustrates shear lag phenomenon where stress on the fibers at the bar's outer surface is greater than on the fibers at the center. In a situation where CFRP bar is being pulled in tension, the surface and core fibers move (slip) in different rates. This is resulting the non-uniform distribution of stress throughout the bar cross-section and hence, affecting its corresponding slip.

5.4. Variation in modulus of elasticity

5.4.1. Failure mode

In the literature, restricted amount of researches has been performed with focusing on the impact of elastic modulus to bond failure mode. Nonetheless, Fig. 23 is plotted to describe the relationship between failure mode and modulus of elasticity by evaluating the indirect data available in the literatures [29,38,39,48,61,63–66,72,75,76,88–94]. It can be clearly noticed from the column chart that bar pullout failure are dominant for all categorized of elastic modulus, accounted about 76% from all specimens. The chart also shows that the experimental data are contributed from CFRP bars having elastic modulus between 100 GPa and 180 GPa. Such modulus of elasticity within the range of 140–160 GPa represents for overall of 78 samples had been failed by pulling out. It implies that CFRP bars with 140–160 GPa modulus of elasticity can provide the desired bond pullout failure.

5.4.2. Bond strength

Further data mined from literatures present the impact of elastic modulus on bond strength as depicted in Fig. 24. The plotted graph have indicated that there is a trend for higher bond strength with increasing modulus of elasticity [47,87,96]. The prime facts is that CFRP bar with higher elastic modulus having more resistant to deform within its elastic range by absorbing more energy [36]. Therefore, higher elastic modulus resulting less slip and subsequently less damage at the CFRP bar's surface [87]. This can result in higher average bond strength as modulus of elasticity increased, as observed in Fig. 24. Moreover, higher in modulus of elasticity may increases the bond stiffness particularly at the ascending function in bond stress-slip model [87]. Nevertheless, limited numbers of investigation have been found to unfold the influence of this parameter on bond performance [47,87].
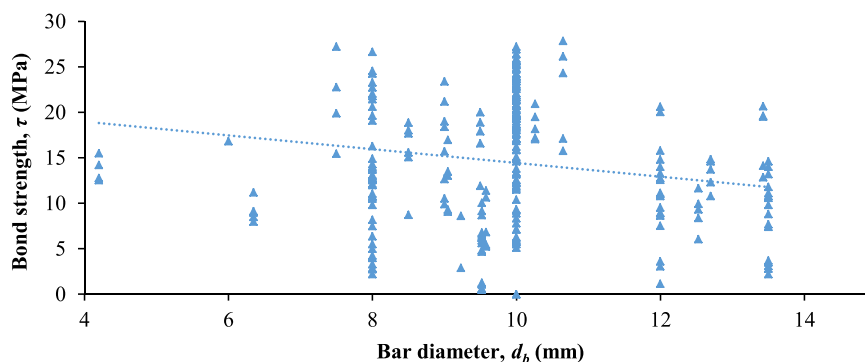
Fig. 20. Relationship between bond strength and bar diameter of CFRP bar [29,38,39,48,61,63–66,72,75,76,88–94].
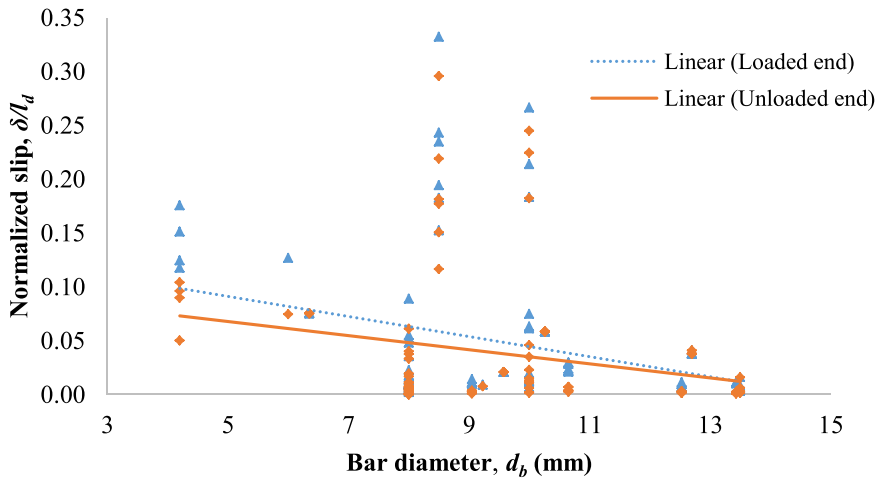
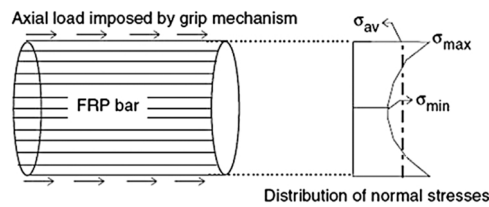**Fig. 21.** Interaction between bar diameter and its corresponding slip [29,38,39,48,61,63–66,72,75,76,88–94].

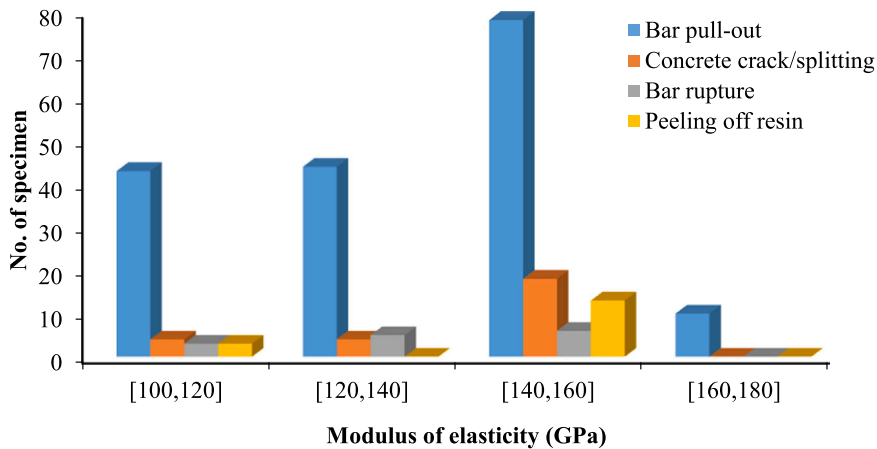**Fig. 22.** Shear lag phenomenon on CFRP bar under pullout force [39,48].

Fig. 23. Relationship between failure mode and modulus of elasticity [29,38,39,48,61,63–66,72,75,76,88–94].

5.5. Effects of surface treatment

5.5.1. Failure mode

The bond strength of concrete embedded with CFRP bars is significantly influenced by bar surface condition. In general, surface treatment can be divided into two categories, namely deformed and non-deformed CFRP bars. The implication of bar surface condition on different failure modes is depicted in Fig. 24. Once again, bar pullout failure were dominant for all type of failure modes followed by concrete split. In bar pullout failure, it is noteworthy that damages on the CFRP bars were either at the bar's interface with concrete or by internal de-bonding of the bar itself. On the other hand, for peeling off resin, non-deformed bars had failed by double the numbers of deformed bar that had been recorded. It can be concluded that peeling off resin were dominant for non-deformed bars with brittle failure at its maximum bond strength and had low residual bond stress [48,62,71,75]. In addition, concrete splitting failure and bar rupture for deformed bars were recorded higher ratio against non-deformed bars.
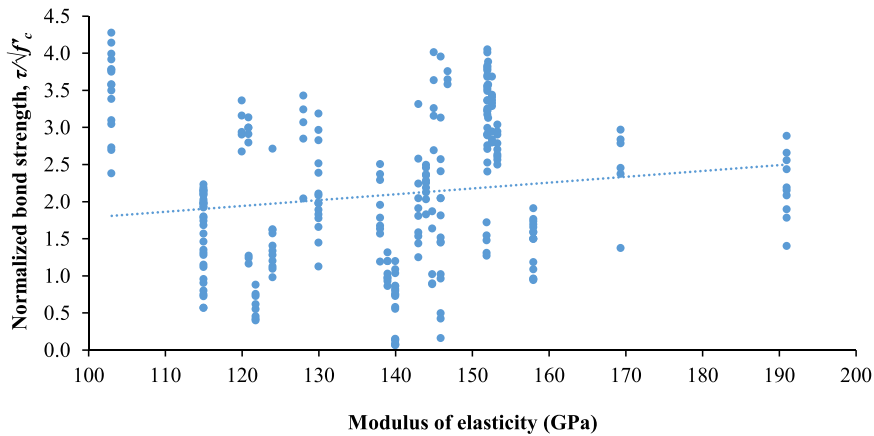
Fig. 24. Effects of modulus of elasticity on bond strength [29,38,39,48,61,63–66,72,75,76,88–94].

5.5.2. Bond strength

In pullout tests, variety of bar surface conditions, including ribbed, helically wrapped, SC, textured and smooth were frequently used as variables. Generally, experimental results on smooth CFRP bar were typically used as a benchmark to observe the impact of having difference surface conditions on bond performance. Fig. 25 provides the valuable information about the implication of difference bar surface conditions on normalized bond strength. There is no doubt that deformed bars which represent by ribbed and spiral wound surface condition had recorded the highest normalized bond strength. They were about 3.0 and 2.6 times higher than normalized bond strength recorded for smooth bars. On the other hand, grooves and textured surface condition were performing better than helically wrapped bars. The mechanisms in transferring the bond stress between concrete and CFRP bars are the main reason for excellent bond performance on deformed bars. Fig. 26 provides an illustration about the mechanisms in transferring the bond stress as unfolded by Pour et al. [57] and Zhang et al. [64]. The mechanisms involved in transferring the bond stress for deformed bar are specifically depend on the geometrical ratios of surface conditions [56,101]. As mentioned by Baena et al. [75], Okelo & Yuan [66] and Hao et al. [101], there are three geometrical ratios considered to evaluate the surface conditions on deformed bar: (i) area to space ratio (a_s); (ii) the relative rib area (R_r); and, (iii) concrete lug ratio (CLR). Fig. 27 depicts all those three geometrical ratios, which can be calculated by performing the Eqs. (11a) to (11c).

$$a_s = \frac{A_r}{r_s} \tag{11a}$$

$$R_r = \frac{A_r}{Pr_s} \tag{11b}$$

$$CLR = \frac{W_c}{W_c + W_f} \tag{11c}$$

where, A_r is the projected rib area (mm²); r_s denotes as rib spacing (mm); P represents the nominal bar perimeter (mm); w_c and w_f are the concrete lug width (mm) and CFRP bar lug width (mm), respectively. The variation in bar surface deformation plays a significant role on bond behavior [39,102]. Based on the investigations revealed by Hao et al. [101] and Malvar et al. [102], the optimum surface
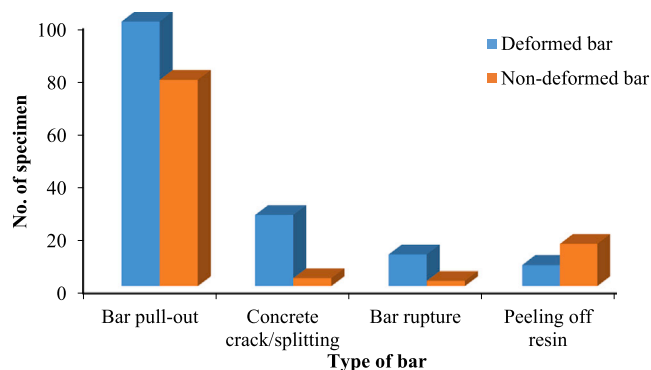

Fig. 25. Effects of surface treatment on the types of failure mode [29,38,39,48,61,63–66,72,75,76,88–94].
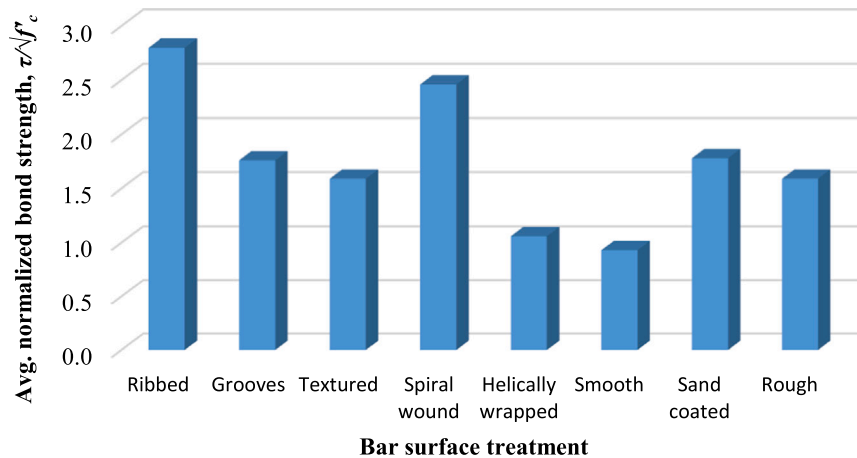
Fig. 26. Impact on bond strength with differences bar surface treatment [29,38,39,48,61,63–66,72,75,76,88–94].
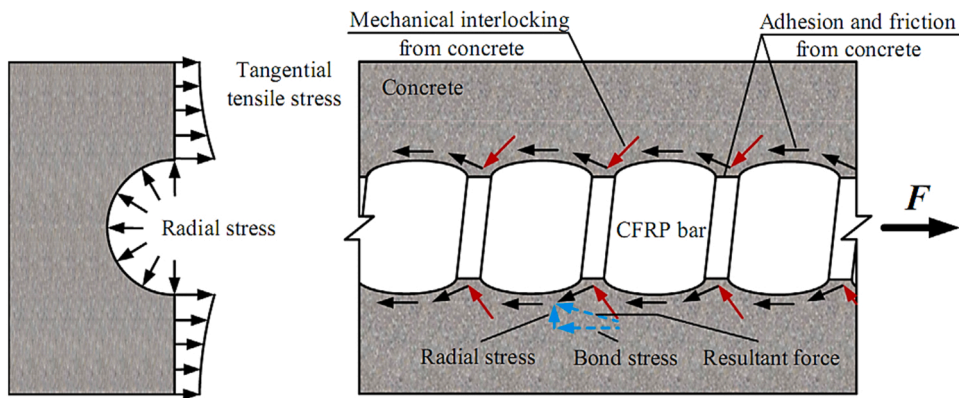

Fig. 27. Mechanisms in transferring the bond stress for embedded concrete with deformed CFRP bars [64].

geometries for deformed FRP bar have been proposed for design references. They have come to the conclusion that the excellent bond strength can be achieved with the rib height is 6% of bar diameter meanwhile, rib spacing is equal to the bar diameter. The R_r value on the other hand, recommended to be 0.06 [101,102].

As for non-deformed bars, CFRP with SC surface exhibit a comparable bond performance against deformed bars with 1.78 of normalized bond strength. This result is 1.9 times higher than normalized bond strength recorded for smooth bars. The only mechanisms in transferring the bond stress for non-deformed bars are chemical adhesion and frictional resistance. Due to the absentee of geometrical ratios, bond strength is also depending on the transverse stress from concrete to enhance the chemical adhesion and frictional resistance [75]. Moreover, considering with no geometrical ratio on smooth CFRP bars, they are not endorsed to be utilized as flexural reinforcement particularly in RC beams unless there are adequate anchoring systems are designed to enhance the bond strength [62,71].

Henceforth, distinct surface condition involves different bond performance of CFRP bars. Yet, surface treatment of CFRP bars is the variable that is not standardized due to its complexity and diversity in its characteristics [62,75]. Throughout the extensive investigations, current researchers had reported that bar's surface treatment contributes an enormous impact on bond strength particularly in the circumstances where the damages had occurred on the bar's surface. For example, Baena et al. [75] had manifested the significant impact of surface treatment on FRP bar's bond strength throughout their 88 direct pullout tests. Also, Esfandeh et al. [37] had concluded with the same agreement that any type of bar's surface treatment resulted in a higher force to pull-out from concrete. Moreover, Solyom & Balázs [62] had studied the effects of 13 different types of bar surface condition on bond strength. They had determined that the bond strength may vary considerably subject to the types of surface treatment but, the bond had significantly improved than steel bars.

The ACI 440.1R-15 [23] have pointed out their concern on bar surface treatment in sustaining the bond strength of embedded concrete with FRP bars. However, ACI 440.1R-15 [23] has not consider any specific variable related to their proposed equation in estimating the bond strength. The other international guidelines as such CSA S806–12 [44], CSA S6–06 [83] and ISIS Canada [24] have proposed a coefficient factor pertaining to the different type of surface conditions in calculating the bond strength, as discussed in Section 4.

5.6. Effect of confinement pressure

Confinement pressure from concrete is another critical parameter that enable CFRP bar to reach its maximum bond strength [23,38, 39]. Transverse reinforcement may provide adequate confinement to concrete. In fact, with the presence of sufficient confinement pressure, it is able to defer or avoid the concrete splitting failure and even increase the bond strength. In addition to that, CFRP bar is expected to fail by pulling out. According to investigation by Zhou et al. [103], they had discovered that as confinement effect increased, the bond strength had increased as well. Moreover, Islam et al. [95] recommend that concrete cover with $2.5d_b$ thickness is satisfactory enough to provide the adequate confinement pressure without failure in concrete cover. (Fig. 28).

Apart from that, preceding researcher like Firas et al. [48] have manifested the impacts of confinement pressure on bond strength for embedded CFRP bars in ultra-high performance fiber-reinforced concrete. However, they have concluded that the bond strength would not necessarily increases along with the increment of confinement pressure (measured by ages of concrete). Also, the experimental results had indicated the maximum bond strength for specimens tested at 3 days and 90 days did not differ significant (by only less than 10% only).

5.7. Effect of bar casting position

This review study further unfolds the implication of bar casting position focusing on two typical cases, namely horizontal and vertical position. The implication of bar casting position on bond strength had been studied by Alunno Rossetti et al. [43], Hossain & Lachemi [104] and Park et al. [105]. All of the authors had carried out a good number of pullout tests on the samples where the bar was set into those two cases. The experimental results indicated a significant impact of bar positioning on bond strength where the bar in horizontal position systematically revealed about 40–91% lower bond strength as compared to vertical position [105]. This phenomenon was reflected by the bleeding and segregation during casting works. They had concluded that during the concreting works, air bubbles and water move upward and being snared beneath the horizontal bar. This, consequently have a detrimental implication on bond strength due to decrease of contact surface between concrete and bars.

5.8. Effect of top-bottom bar

This review study continued to clarifies the effect of top-bottom bar particularly related to the bar arrangement in RC beam. Hossain & Lachemi [104] and Park et al. [105] had conducted the pullout tests with regard to the top and bottom FRP bars positioning as the main variable. By comparing the test results for top and bottom bars, it had shown top bars exhibited lower bond strength where about only 45% to that of bottom bars [105]. This was also mainly due to bleeding and segregation effects during casting works. However, these effects were only validated with the application of normal concrete where it was laid in multiple layers and extensive mechanical vibration had been applied for the purpose of compactions. In the application of self-compacting concrete [104], the impact on bleeding and segregation effects were observed to be less significant on the top and bottom bar. Therefore, the different of bond strength due to top-bottom bar factor were reduced significantly. Henceforth, CSA S806–12 [44], CSA S6–06 [83] and ISIS Canada [24] recommend to use two different values for bar location (*K1*) either 1.3 or 1.0 as a modification factor. This is briefly discussed in Section 4.

6. Recommended research areas for future studies

Having performing this critical review, new significant variation of CFRP bars are being developed every year, improving its material characteristics. Hence, numerous hotspot research areas were identified for further considerations and to be shortlisted as research topics in future studies.

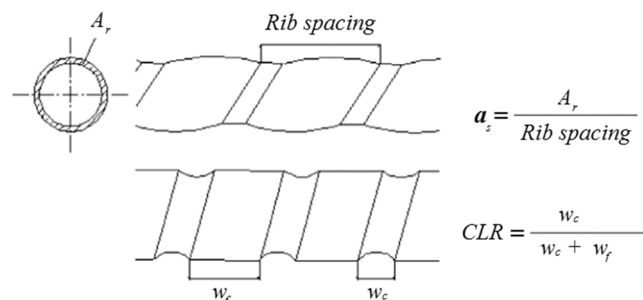a) Bond strength of CFRP bar with additional anchorage system embedded in concrete:

$$a_s = \frac{A_r}{Rib\ spacing}$$

$$CLR = \frac{w_c}{w_c + w_f}$$

Fig. 28. Definition of geometrical ratios on the deformed CFRP bar [75].

- In the past 20 years, CFRP bars have attracted overwhelming attention for researchers to conduct investigations with the objective to enhance the bond strength and its performances in concrete. The frequent variables involved in the research consist of change the inherent properties of CFRP bar. These include bar diameter, modulus of elasticity and surface configurations [29,38,39,48,61, 63–66,72,75,76,88–94].
- However, in the last 5 years, with the current technology, CFRP bars literally attract more attention for researchers to investigate the possibility to develop and increase the bond strength for CFRP bars with additional anchorage or hooked-end [61,64,93,106].
- Additional research is necessary to fully understand regarding the respond and bond performance of new available CFRP bar with additional anchorage system embedded in concrete. The improvement in bond performance would validate the CFRP bar with additional anchorage to be applied on RC and pre-stressed structures as well [107].

a) Arrangement and configuration CFRP bar with additional anchorage system:

- The development of new additional anchorage system or hooked-end [61,64,93,106] on CFRP bar would change their existing well-known behavior in concrete particularly on the bar arrangement and configuration. These include concrete cover, bar spacing, development length and modification factor for bar positioning in the member (top-bottom bar). For the sake of clarification, further investigations are required to observe their responds with respect to these variables.

a) Behavior of CFRP bar with additional anchorage in different types of concrete:

1. Fibers in concrete: Presence of fibers in concrete may improve the mechanical properties particularly in tensile strength due to the bridging effects [108–111]. Other than that, the impacts of fibers addition in concrete are able to prevent the wider crack widths as well as provide additional confinement pressure to CFRP bar. The types of fiber added in concrete include steel, PVA, aramid, polypropylene and glass fiber.
2. Geopolymer concrete: The bond performance of embedded CFRP bars in geopolymer concrete recently has only been the subject for few studies. High performance and sustainable structures might be the outcomes by combination of these two materials. For example, the applications of CFRP bar as flexural reinforcement in RC beam has great potential, according to investigation by Ahmed et al. [112]. However, they observed that the CFRP bars had failed by de-bonding failure from the concrete beam due to insufficient bonding. Hence, it is crucial to conduct investigations on bond behavior of CFRP bar embedded in geopolymer concrete.

7. Conclusions

Fiber-reinforced polymer (FRP) bars are being acknowledged as an alternate remedy for civil infrastructure degradation. One of these FRP is CFRP bars that have gained popularity because to their excellent corrosion resistance, cost-effectiveness, design flexibility, and low maintenance requirements. The bond properties of embedded CFRP bar in concrete seems to be the most important aspect for the material's use to corrosion-free concrete structures. CFRP materials, unlike metallic reinforcements have exceptional tensile strength, linear elastic characteristics, anisotropic, noncorrosive and nonmagnetic materials which might consequence in a distinct force transmission mechanism between concrete and reinforcement bar. This research conducts a complete evaluation concentrating on the bond strength to cover the remarkable contributions related to bond performance in previous studies. Following a thorough review of the literatures, numerous conclusions regarding the bond performance of embedded CFRP bars in concrete can be successfully drawn:

1. Pullout test has been extensively adapted method in determining the bond strength of embedded CFRP bars in concrete. It offers an economical, usability and practicality in evaluating the bond strength behavior.
2. The BPE modified model, CMR model and Tighiouart et al. model have relatively proposed the simple form of bond stress-slip model with reliable results. However, CMR model and Tighiouart et al. model only consider the ascending curve where it is suitable for the analysis at serviceability state level. The modified BPE model has been identified to be the most appropriate and practical model. Nevertheless, it has attracted great interest of using CMR model as a replacement for the ascending stage to assess the complete bond stress-slip behavior.
3. Bond strength prediction analysis have found that ACI 440.1R-15 and JSCE underestimate the bond strength. Whilst, CSA S806-12 and CSA S6-06 & ISIS Canada overestimate the bond strength by 20% and 24%, respectively. In general, predicting values of bond strength by international guidelines are conservative. This can be attributed to the number of factors considered in those equations.
4. Throughout the statistical measures, bond strength prediction by ACI 440.1R-15 is discovered to be more realistic as compared to the experimental results.
5. Over 273 specimens of CFRP bar involved in pullout tests were extracted from the experimental works in literatures. They were analyzed systematically and presented in an extensive review concentrating on the major factors affecting the bond strength. Those major factors were recognized and quantitatively analyzed to fully comprehend their responds in concrete. Precisely, the factors like inherent properties of CFRP bar (include diameter, elastic modulus and surface condition), inherent concrete properties (include compressive strength) as well as bar arrangement and configuration (include embedment length, bar casting position and top-bottom bar) literally affect the CFRP bond behavior and performance.

6. In addition to that, the compressive strength, bar diameter and elastic modulus are the three major factors that have linear relationships with the bond strength. Nonetheless, the bond strength was identified to have a nonlinear relationship against the embedment length.

7. Hotspot research areas were also identified for further considerations in future studies. They were including the possibility to develop and increase the bond strength for CFRP bars with additional anchorage, the new arrangement and configuration of CFRP bar with additional anchorage system and the characteristics behavior of CFRP bar with additional anchorage in different types of concrete. The discoveries of these new parameters will enhance the excitement in employing the CFRP bars as structural reinforcement in RC structures.

In brief, the main findings of this review will help the scientists, structural engineers and practitioners in understanding the important aspects of bond dependent-factors for embedded CFRP bars in concrete. The employment of CFRP bars as structural reinforcement for RC structures is a step towards establishing such smart and flexible construction schemes.

Declaration of Competing Interest

The authors declare that they have no known competing financial interests or personal relationships that could have appeared to influence the work reported in this paper.

Data Availability

Data will be made available on request.

Acknowledgements

References

[1] M. Basdeki, C. Apostolopoulos, The effect of shot blasting process on mechanical properties and anti-corrosive behavior of steel reinforcement, Metals 12 (2022), https://doi.org/10.3390/met12020275.

[2] X. Wang, Z. Jin, J. Liu, F. Chen, P. Feng, J. Tang, Research on internal monitoring of reinforced concrete under accelerated corrosion, using XCT and DIC technology, Constr. Build. Mater. 266 (2021), https://doi.org/10.1016/j.conbuildmat.2020.121018.

[3] S. Fonna, I. Bin, M. Ibrahim, Gunawarman, S. Huzni, M. Ikhsan, S. Thalib, Investigation of corrosion products formed on the surface of carbon steel exposed in Banda Aceh's atmosphere, Heliyon 7 (2021), https://doi.org/10.1016/j.heliyon.2021.e06608.

[4] U.M. Angst, Challenges and opportunities in corrosion of steel in concrete, Mater. Struct. Constr. 51 (2018) 1–20, https://doi.org/10.1617/s11527-017-1131-6.

[5] R. Cabrera-Sierra, E. Sosa, M.T. Oropeza, I. González, Electrochemical study on carbon steel corrosion process in alkaline sour media, Electrochim. Acta 47 (2002) 2149–2158, https://doi.org/10.1016/S0013-4686(02)00090-7.

[6] P. Refait, A.-M. Grolleau, M. Jeannin, C. Rémazeilles, R. Sabot, Corrosion of carbon steel in marine environments: role of the corrosion product layer, Corros. Mater. Degrad. 1 (2020) 198–218, https://doi.org/10.3390/cmd1010010.

[7] K. Bhargava, A.K. Ghosh, Y. Mori, S. Ramanujam, Corrosion-induced bond strength degradation in reinforced concrete-Analytical and empirical models, Nucl. Eng. Des. 237 (2007) 1140–1157, https://doi.org/10.1016/j.nucengdes.2007.01.010.

[8] A. Paul, Spalling of Concrete - Causes, Prevention and Repair, Civ. Digit. Website. (2014) 6 (access: August 13, 2022).

[9] M. Arockiasamy, S. Chidambaram, A. Amer, M. Shahawy, Time-dependent deformations of concrete beams reinforced with CFRP bars, Compos. Part B Eng. 31 (2000) 577–592, https://doi.org/10.1016/S1359-8368(99)00045-1.

[10] I.F. Kara, A.F. Ashour, M.A. Köroğlu, Flexural behavior of hybrid FRP/steel reinforced concrete beams, Compos. Struct. 129 (2015) 111–121, https://doi.org/10.1016/j.compstruct.2015.03.073.

[11] A. Siddika, M.A. Al Mamun, R. Alyousef, Y.H.M. Amran, Strengthening of reinforced concrete beams by using fiber-reinforced polymer composites: a review, J. Build. Eng. 25 (2019), https://doi.org/10.1016/j.jobe.2019.100798.

[12] Y.H. Mugahed Amran, R. Alyousef, R.S.M. Rashid, H. Alabduljabbar, C.C. Hung, Properties and applications of FRP in strengthening RC structures: a review, Structures 16 (2018) 208–238, https://doi.org/10.1016/j.istruc.2018.09.008.

[13] M.R. El-Zeadani, M.R. Raizal Saifulnaz, Y.H. Mugahed Amran, F. Hejazi, M.S. Jaafar, R. Alyousef, H. Alabduljabbar, Analytical mechanics solution for measuring the deflection of strengthened RC beams using FRP plates, Case Stud. Constr. Mater. 11 (2019), https://doi.org/10.1016/j.cscm.2019.e00272.

[14] M. El-Zeadani, M.R. Raizal Saifulnaz, F. Hejazi, Y.H. Mugahed Amran, M.S. Jaafar, R. Alyousef, F. Alrshoudi, Mechanics-based approach for predicting the short-term deflection of CFRP plated RC beams, Compos. Struct. 225 (2019), https://doi.org/10.1016/j.compstruct.2019.111169.

[15] Y.H.M. Amran, R. Alyousef, H. Alabduljabbar, A. Alaskar, F. Alrshoudi, Properties and water penetration of structural concrete wrapped with CFRP, Results Eng. 5 (2020), https://doi.org/10.1016/j.rineng.2019.100094.

[16] N.I. Rahim, B.S. Mohammed, A. Al-Fakih, M.M.A. Wahab, M.S. Liew, A. Anwar, Y.H.Mugahed Amran, Strengthening the structural behavior of web openings in RC deep beam using CFRP, Materials 13 (2020) 1–21, https://doi.org/10.3390/ma13122804.

[17] M. Basri, C. Bakar, R. Saifulnaz, M. Rashid, M. Amran, M.S. Jaafar, N.I. Vatin, R. Fediuk, Flexural strength of concrete beam reinforced with CFRP bars: a review, Materials 15 (2022) 1–21.

[18] M. El-Zeadani, R.S.M. Rashid, M.Y.H. Amran, M.I. Swi, Effect of the plate bondstress-slip property on the flexural strength of FRP Plated RC beams using a displacement-based approach, SN Appl. Sci. 2 (2020), https://doi.org/10.1007/s42452-020-03723-w.

[19] M. El-Zeadani, M.R.R. Saifulnaz, Y.H. Mugahed Amran, F. Hejazi, M.S. Jaafar, R. Alyousef, H. Alabduljabbar, Flexural strength of FRP plated RC beams using a partial-interaction displacement-based approach, Structures 22 (2019) 405–420, https://doi.org/10.1016/j.istruc.2019.09.008.

[20] M. El-Zeadani, M.R. Raizal Saifulnaz, M. Amran, Full-range bondstress-slip model for externally bonded FRP plates including a frictional component, Compos. Struct. 262 (2021), https://doi.org/10.1016/j.compstruct.2020.113372.

[21] A. Al-Nini, E. Nikbakht, A. Syamsir, N. Shafiq, B.S. Mohammed, A. Al-Fakih, W. Al-Nini, Y.H.M. Amran, Flexural behavior of double-skin steel tube beams filled with fiber-reinforced cementitious composite and strengthened with CFRP sheets, Materials 13 (2020), https://doi.org/10.3390/ma13143064.

[22] L.C. Hollaway, A review of the present and future utilisation of FRP composites in the civil infrastructure with reference to their important in-service properties, Constr. Build. Mater. 24 (2010) 2419–2445, https://doi.org/10.1016/j.conbuildmat.2010.04.062.

[23] ACI 440.1R-15, Guide for the design and construction of structural concrete reinforced with Firber-Reinforced Polymer (FRP) bars, 2015.

[24] ISIS Canada (2007), Reinforcing Concrete Structures with Fibre Reinforced Polymers Reinforcing Concrete Structures with Fibre Reinforced Polymers-Design manual No. 3, Manitoba, Canada, 2007.

[25] A. Zaman, S.A. Gutub, M.A. Wafa, A review on FRP composites applications and durability concerns in the construction sector, J. Reinf. Plast. Compos 32 (2013) 1966–1988, https://doi.org/10.1177/0731684413492868.

[26] R.J. Gravina, S.T. Smith, Flexural behaviour of indeterminate concrete beams reinforced with FRP bars, Eng. Struct. 30 (2008) 2370–2380, https://doi.org/10.1016/j.engstruct.2007.12.019.

[27] X. Lin, Y.X. Zhang, Bond-slip behaviour of FRP-reinforced concrete beams, Constr. Build. Mater. 44 (2013) 110–117, https://doi.org/10.1016/j.conbuildmat.2013.03.023.

[28] M. Bocciarelli, M.A. Pisani, Modified force method for the nonlinear analysis of FRP reinforced concrete beams, Compos. Struct. 131 (2015) 645–653, https://doi.org/10.1016/j.compstruct.2015.05.075.

[29] J.A. Rami Hamad, M.A. Megat Johari, R.H. Haddad, Mechanical properties and bond characteristics of different fiber reinforced polymer rebars at elevated temperatures, Constr. Build. Mater. 142 (2017) 521–535, https://doi.org/10.1016/j.conbuildmat.2017.03.113.

[30] L. Wang, J. Zhang, W. Chen, F. Fu, K. Qian, Short term crack width prediction of CFRP bars reinforced coral concrete, Eng. Struct. 218 (2020), 110829, https://doi.org/10.1016/j.engstruct.2020.110829.

[31] P. Cousin, M. Hassan, P.V. Vijay, M. Robert, B. Benmokrane, Chemical resistance of carbon, basalt, and glass fibers used in FRP reinforcing bars, J. Compos. Mater. 53 (2019) 3651–3670, https://doi.org/10.1177/0021998319844306.

[32] F. Ceroni, E. Cosenza, M. Gaetano, M. Pecce, Durability issues of FRP rebars in reinforced concrete members, Cem. Concr. Compos. 28 (2006) 857–868, https://doi.org/10.1016/j.cemconcomp.2006.07.004.

[33] N.H.F.A. Halim, S.C. Alih, M. Vafaei, M. Baniahmadi, A. Fallah, Durability of fibre reinforced polymer under aggressive environment and severe loading: a review, Int. J. Appl. Eng. Res. 12 (2017) 12519–12533.

[34] F. Micelli, A. Nanni, Durability of FRP rods for concrete structures, Constr. Build. Mater. 18 (2004) 491–503, https://doi.org/10.1016/j.conbuildmat.2004.04.012.

[35] R. Verma, O.P. Netula, Carbon fiber as a construction material, Imp. J. Interdiscip. Res. 3 (2017) 1218–1220.

[36] B. Başaran, İ. Kalkan, A. Beycioğlu, I. Kasprzyk, A review on the physical parameters affecting the bond behavior of FRP bars embedded in concrete, Polymers 14 (2022), https://doi.org/10.3390/polym14091796.

[37] M. Esfandeh, A.R. Sabet, A.M. Rezadoust, M.B. Alavi, Bond performance of FRP rebars with various surface deformations in reinforced concrete, Polym. Compos. (2009) 576–582, https://doi.org/10.1002/pc.

[38] F. AL-mahmoud, A. Castel, R. François, C. Tourneur, Effect of surface pre-conditioning on bond of carbon fibre reinforced polymer rods to concrete, Cem. Concr. Compos. 29 (2007) 677–689, https://doi.org/10.1016/j.cemconcomp.2007.04.010.

[39] Z. Achillides, K. Pilakoutas, Bond behavior of fiber reinforced polymer bars under direct pullout conditions, J. Compos. Constr. 8 (2004) 173–181, https://doi.org/10.1061/(asce)1090-0268(2004)8:2(173).

[40] Z. Achillides, K. Pilakoutas, M. Guadagnini, P. Waldron, Tests for the evaluation of bond properties of FRP bars in concrete, FRP Compos. Civ. Eng. - CICE 2004 (2004) 343–350, https://doi.org/10.1201/9780203970850.ch37.

[41] R. Eligehausen, E. Popov, V. Bertero, Local bond stress-slip relationships of deformed bars under generalized excitations, in: Proc. 7th Eur. Conf. Earthq. Eng. Vol. 4. Athens Techn. Chamb. Greece, 1982, S. 69–80, 1982: pp. 69–80.

[42] L.J. Malvar, Bond stress-slip characteristics of FRP bars, 1994.

[43] V.A. Rossetti, D. Galeota, M.M. Giammatteo, Local bond stress-slip relationships of glass fibre reinforced plastic bars embedded in concrete, Mater. Struct. 28 (1995) 340–344, https://doi.org/10.1007/BF02473149.

[44] CSA S806–12, Design and construction of building structures with fibre-reinforceds, Canadian Standards Association, Mississauga, Ontario, Canada, 2012.

[45] F. Yan, Z. Lin, M. Yang, Bond mechanism and bond strength of GFRP bars to concrete: a review, Compos. Part B 98 (2016) 56–69, https://doi.org/10.1016/j.compositesb.2016.04.068.

[46] W. Wei, F. Liu, Z. Xiong, Z. Lu, L. Li, Bond performance between fibre-reinforced polymer bars and concrete under pull-out tests, Constr. Build. Mater. 227 (2019), https://doi.org/10.1016/j.conbuildmat.2019.116803.

[47] Amnon Katzl, Bond to concrete of FRP rebars and tendons, Compos. Constr. (2001) 121–129.

[48] S.A. Firas, F. Gilles, L.R. Robert, Bond between carbon fibre-reinforced polymer (CFRP) bars and ultra high performance fibre reinforced concrete (UHPFRC): experimental study, Constr. Build. Mater. 25 (2011) 479–485, https://doi.org/10.1016/j.conbuildmat.2010.02.006.

[49] M.M. Rafi, A. Nadjai, F. Ali, D. Talamona, Aspects of behaviour of CFRP reinforced concrete beams in bending, Constr. Build. Mater. 22 (2008) 277–285, https://doi.org/10.1016/j.conbuildmat.2006.08.014.

[50] M.M. Rafi, A. Nadjai, F. Ali, Experimental testing of concrete beams reinforced with carbon FRP bars, J. Compos. Mater. 41 (2007) 2657–2673, https://doi.org/10.1177/0021998307078727.

[51] H.L. Lye, B.S. Mohammed, M.M.A. Wahab, M.S. Liew, Bond relationship of carbon fiber-reinforced polymer (Cfrp) strengthened steel plates exposed to service temperature, Materials 14 (2021), https://doi.org/10.3390/ma14133761.

[52] F. Ellert, I. Bradshaw, R. Steinhilper, Major factors influencing tensile strength of repaired CFRP-samples, Procedia CIRP (2015) 275–280, https://doi.org/10.1016/j.procir.2015.06.049.

[53] A. Vahedian, R. Shrestha, K. Crews, Modelling of factors affecting bond strength of fibre reinforced polymer externally bonded to timber and concrete, Int. J. Struct. Constr. Eng. 11 (2017), https://doi.org/10.1999/1307-6892/10008338.

[54] E. Toumpanaki, J.M. Lees, G.P. Terrasi, Bond durability of carbon fiber–reinforced polymer tendons embedded in high-strength concrete, J. Compos. Constr. 22 (2018), https://doi.org/10.1061/(asce)cc.1943-5614.0000870.

[55] E. Toumpanaki, J.M. Lees, G.P. Terrasi, Analytical predictive model for the long-term bond performance of CFRP tendons in concrete, Compos. Struct. 250 (2020), https://doi.org/10.1016/j.compstruct.2020.112614.

[56] E. Cosenza, G. Manfredi, R. Realfonzo, Development length of FRP straight rebars, Compos. Part B Eng. 33 (2002) 493–504, https://doi.org/10.1016/S1359-8368(02)00051-3.

[57] S.M. Pour, M.S. Alam, A.S. Milani, Improved bond equations for fiber-reinforced polymer bars in concrete, Materials 9 (2016) 1–14, https://doi.org/10.3390/ma9090737.

[58] ACI 440.3R-12, Guide Test Methods for Fiber-Reinforced Polymers (FRPs) for Reinforcing or Strengthening Concrete Structures, 2012.

[59] BS EN 10080:2005, Steel for the reinforcement of concrete - Weldable reinforcing steel - General, 2005.

[60] M.B. Muñoz, Study of Bond Behaviour Between FRP Reinforcement and Concrete, PhD thesis, University of Girona, Spain, 2010.

[61] Q. Wang, H. Zhu, Y. Tong, W. Su, P. Zhang, Bond-slip behaviour of the CFRP ribbed bars anchored with the innovative additional ribs in concrete, Compos. Struct. 262 (2021), 113595, https://doi.org/10.1016/j.compstruct.2021.113595.

[62] S. Solyom, G.L. Balázs, Bond of FRP bars with different surface characteristics, Constr. Build. Mater. 264 (2020), 119839, https://doi.org/10.1016/j.conbuildmat.2020.119839.

[63] M. Caro, Y. Jemaa, S. Dirar, A. Quinn, Bond performance of deep embedment FRP bars epoxy-bonded into concrete, Eng. Struct. 147 (2017) 448–457, https://doi.org/10.1016/j.engstruct.2017.05.069.

[64] B. Zhang, H. Zhu, G. Wu, Q. Wang, T. Li, Improvement of bond performance between concrete and CFRP bars with optimized additional aluminum ribs anchorage, Constr. Build. Mater. 241 (2020), 118012, https://doi.org/10.1016/j.conbuildmat.2020.118012.

[65] Y.H. Lee, M.S. Kim, H. Kim, J. Lee, D.J. Kim, Experimental study on bond strength of fiber reinforced polymer rebars in normal strength concrete, J. Adhes. Sci. Technol. 27 (2013) 508–522, https://doi.org/10.1080/01694243.2012.687554.

[66] R. Okelo, R.L. Yuan, Bond strength of fiber reinforced polymer rebars in normal strength concrete, Constr. Build. Mater. 9 (2005) 203–213, https://doi.org/10.1061/(ASCE)1090-0268(2005)9:3(203).

[67] J.Y. Lee, T.Y. Kim, T.J. Kim, C.K. Yi, J.S. Park, Y.C. You, Y.H. Park, Interfacial bond strength of glass fiber reinforced polymer bars in high-strength concrete, Compos. Part B Eng. 39 (2008) 258–270, https://doi.org/10.1016/j.compositesb.2007.03.008.

[68] ASTM D7205/D7205M, Standard Test Method for Tensile Properties of Fiber Reinforced Polymer Matrix, i (2016). https://doi.org/10.1520/D7205.

[69] ASTM C192/C192M − 15, Standard Practice for Making and Curing Concrete Test Specimens in the Laboratory, 2015. https://doi.org/10.1520/C0192.

[70] ASTM-C511–13, Standard Specification for Mixing Rooms, Moist Cabinets, Moist Rooms, and Water, ASTM Stand. Guid. (2006) 23–25.

[71] E. Cosenza, G. Manfredi, R. Realfonzo, Behavior and modeling of bond of FRP rebars to concrete, J. Compos. Constr. 1 (1997) 40–51, https://doi.org/10.1061/(asce)1090-0268(1997)1:2(40).

[72] V. Calvet, M. Valcuende, J. Benlloch, J. Cánoves, Influence of moderate temperatures on the bond between carbon fibre reinforced polymer bars (CFRP) and concrete, Constr. Build. Mater. 94 (2015) 589–604, https://doi.org/10.1016/j.conbuildmat.2015.07.053.

[73] H. Wang, A. Belarbi, Static and fatigue bond characteristics of FRP rebars embedded in fiber-reinforced concrete, J. Compos. Mater. 44 (2010) 1605–1622, https://doi.org/10.1177/0021998309355845.

[74] W.H. Soong, J. Raghavan, S.H. Rizkalla, Fundamental mechanisms of bonding of glass fiber reinforced polymer reinforcement to concrete, Constr. Build. Mater. 25 (2011) 2813–2821, https://doi.org/10.1016/j.conbuildmat.2010.12.054.

[75] M. Baena, L. Torres, A. Turon, C. Barris, Experimental study of bond behaviour between concrete and FRP bars using a pull-out test, Compos. Part B Eng. 40 (2009) 784–797, https://doi.org/10.1016/j.compositesb.2009.07.003.

[76] M.A. Aiello, M. Leone, M. Pecce, Bond performances of FRP rebars-reinforced concrete, J. Mater. Civ. Eng. 19 (2007) 205–213.

[77] E. Cosenza, G. Manfredi, R. Realfonzo, Analytical modelling of bond between FRP reinforcing bars and concrete, in: L. Taerwe (Ed.), Non-Metallic Reinf. Concr. Struct. Proc. Second Int. RILEM Symp., E & FN Spon, London, 1995: pp. 164–171.

[78] B. Tighiouart, B.U. Benmokrane, D. Gao, Investigation of bond in concrete member with fibre reinforced.pdf, Constr. Build. Mater. 12 (1998) 453–462.

[79] X. Lin, Y.X. Zhang, Evaluation of bond stress-slip models for FRP reinforcing bars in concrete, Compos. Struct. 107 (2014) 131–141, https://doi.org/10.1016/j.compstruct.2013.07.037.

[80] R. Masmoudi, A. Masmoudi, M. Ben Ouezdou, A. Daoud, Long-term bond performance of GFRP bars in concrete under temperature ranging from 20 °C to 80 °C, Constr. Build. Mater. 25 (2011) 486–493, https://doi.org/10.1016/j.conbuildmat.2009.12.040.

[81] FIB, Bond of reinforcement in concrete, State-of-art Report, Bulletin 10, fib-International Federation for Concrete Task Group Bond Models, Lausanne, Switzerland, 2000.

[82] B. Wambeke, C. Shield, Development length of glass fiber reinforced polymer bars in concrete, Acids Struct. J. 103 (2006) 11–17.

[83] CSA-S6–06, Canadian Highway Bridge Design Code, Canadian Standards Association, Mississauga, Ontario, Canada, 2006.

[84] M. A, U. T, Recommendation for design and construction of concrete structures using continuous fiber reinforcing materials, 1997.

[85] M.S.Alam Md Shahnewaz, Improved shear equations for steel fiber-reinforced concrete deep and slender beams, Acids Struct. J. 111 (2014), https://doi.org/10.14359/51686736.

[86] D.C. Montgomery, Design and Analysis of Experiments, John Wiley & Sons, Hoboken, NJ, USA, 2008.

[87] S. Solyom, M. Di Benedetti, A. Szijártó, G.L. Balázs, Non-metallic reinforcements with different moduli of elasticity and surfaces for concrete structures, Archit. Civ. Eng. Environ. 11 (2018) 79–88, https://doi.org/10.21307/acee-2018-025.

[88] B. Benmokrane, B. Zhang, K. Laoubi, B. Tighiouart, I. Lord, Mechanical and bond properties of new generation of carbon fibre reinforced polymer reinforcing bars for concrete structures, Can. J. Civ. Eng. 29 (2002) 338–343, https://doi.org/10.1139/l02-013.

[89] G. Thiagarajan, Experimental and analytical behavior of carbon fiber-based rods as flexural reinforcement, J. Compos. Constr. 7 (2003) 64–72, https://doi.org/10.1061/(asce)1090-0268(2003)7:1(64).

[90] J.P. Won, C.G. Park, H.H. Kim, S.W. Lee, C. Il Jang, Effect of fibers on the bonds between FRP reinforcing bars and high-strength concrete, Compos. Part B Eng. 39 (2008) 747–755, https://doi.org/10.1016/j.compositesb.2007.11.005.

[91] Z. Dong, G. Wu, B. Xu, X. Wang, L. Taerwe, Bond performance of alkaline solution pre-exposed FRP bars with concrete, Mag. Concr. Res. 70 (2018) 894–904, https://doi.org/10.1680/jmacr.17.00027.

[92] A. Rolland, M. Quiertant, A. Khadour, S. Chataigner, K. Benzarti, P. Argoul, Experimental investigations on the bond behavior between concrete and FRP reinforcing bars, Constr. Build. Mater. 173 (2018) 136–148, https://doi.org/10.1016/j.conbuildmat.2018.03.169.

[93] T. Li, H. Zhu, Q. Wang, J. Li, T. Wu, Experimental study on the enhancement of additional ribs to the bond performance of FRP bars in concrete, Constr. Build. Mater. 185 (2018) 545–554, https://doi.org/10.1016/j.conbuildmat.2018.06.198.

[94] J. Zhao, X. Li, X. Zhang, Experimental and theoretical research on bond performance between CFRP bar and concrete under monotonic and reversed cyclic loading, Eng. Struct. 246 (2021), 112994, https://doi.org/10.1016/j.engstruct.2021.112994.

[95] S. Islam, H.M. Afefy, K. Sennah, H. Azimi, Bond characteristics of straight- and headed-end, ribbed-surface, GFRP bars embedded in high-strength concrete, Constr. Build. Mater. 83 (2015) 283–298, https://doi.org/10.1016/j.conbuildmat.2015.03.025.

[96] S. Sólyom, G.L. Balázs, Influence of FRC on bond characteristics of FRP reinforcement, Proc. 11th Fib Int. PhD Symp. Civ. Eng. FIB 2016. (2016) 271–278.

[97] A. Borosnyói, Influence of service temperature and strain rate on the bond performance of CFRP reinforcement in concrete, Compos. Struct. 127 (2015) 18–27, https://doi.org/10.1016/j.compstruct.2015.02.076.

[98] F. Focacci, A. Nanni, C.E. Bakis, Local bond-slip relationship for FRP reinforcement in concrete, J. Compos. Constr. 4 (1) (2000) 24–31.

[99] R. Kotynia, D. Szczech, M. Kaszubska, Bond behavior of GRFP bars to concrete in beam test, Procedia Eng. 193 (2017) 401–408, https://doi.org/10.1016/j.proeng.2017.06.230.

[100] M. Abedini, E. Akhlaghi, J. Mehrmashhadi, M.H. Mussa, M. Ansari, T. Momeni, Evaluation of concrete structures reinforced with fiber reinforced polymers bars: a review, J. Asian Sci. Res 7 (2017) 165–175, https://doi.org/10.18488/journal.2.2017.75.165.175.

[101] Q. Hao, Y. Wang, Z. He, J. Ou, Bond strength of glass fiber reinforced polymer ribbed rebars in normal strength concrete, Constr. Build. Mater. 23 (2009) 865–871, https://doi.org/10.1016/j.conbuildmat.2008.04.011.

[102] L.J. Malvar, J.V. Cox, K.B. Cochran, Bond between carbon fiber reinforced polymer bars and concrete, I: Exp. Study 7 (2003) 154–163.

[103] Y. Zhou, G. Wu, L. Li, Z. Guan, M. Guo, L. Yang, Z. Li, Experimental investigations on bond behavior between FRP Bars and advanced sustainable concrete, Polymers 14 (2022) 1–17.

[104] K.M.A. Hossain, M. Lachemi, Bond behavior of self-consolidating concrete with mineral and chemical admixtures, J. Mater. Civ. Eng. 20 (2008) 608–616, https://doi.org/10.1061/(asce)0899-1561(2008)20:9(608).

[105] J.-S. Park, A.-R. Lim, J. Kim, Jung-Yoon Lee, Bond performance of fiber-reinforced polymer rebars in different casting positions, Polym. Compos. 37 (2016) 2098–2108, https://doi.org/10.1002/pc.

[106] J.W. Schmidt, A. Bennitz, B. Täljsten, P. Goltermann, H. Pedersen, Mechanical anchorage of FRP tendons – a literature review, Constr. Build. Mater. 32 (2012) 110–121, https://doi.org/10.1016/j.conbuildmat.2011.11.049.

[107] H. Zhu, Q. Wang, J. Dai, C. Wang, G. Wu, Innovative additional aluminum alloy ribs anchorage for improving the bond reliability of pretensioned CFRP bar: a feasibility study, Compos. Struct. 280 (2022), 114817, https://doi.org/10.1016/j.compstruct.2021.114817.

[108] M.V. Mohod, Performance of steel fiber reinforced concrete, Int. J. Eng. Sci. ISSN 1 (2012) 1–4.

[109] A.M. Shende, A.M. Pande, M.G. Pathan, Experimental study on steel fiber reinforced concrete for M-40 grade, Int. Ref. J. Eng. Sci. 1 (2012) 43–48.

[110] I.S. Ibrahim, M.B.Che Bakar, Effects on mechanical properties of industrialised steel fibres addition to normal weight concrete, Procedia Eng. 14 (2011) 2616–2626, https://doi.org/10.1016/j.proeng.2011.07.329.

[111] S. Junmin, Z. Yancong, Fiber-reinforced mechanism and mechanical performance of composite fibers reinforced concrete, J. Wuhan. Univ. Technol. Sci. Ed. 35 (2020) 121–130.

[112] H.Q. Ahmed, D.K. Jaf, S.A. Yaseen, Comparison of the flexural performance and behaviour of Fly-ash-based geopolymer concrete beams reinforced with CFRP and GFRP bars, Adv. Mater. Sci. Eng. (2020)) (2020), https://doi.org/10.1155/2020/3495276.